Food and Chemical Toxicology 164 (2022) 113012

Contents lists available at ScienceDirect

Food and Chemical Toxicology

journal homepage: www.elsevier.com/locate/foodchemtox

In vitro toxicity of glyphosate in Atlantic salmon evaluated with a 3D hepatocyte-kidney co-culture model

L. Søfteland [a,*], P.A. Olsvik [a,b]

[a] Institute of Marine Research, Nordnesgaten 50, 5005, Bergen, Norway
[b] Nord University, Universitetsalléen 11, 8049, Bodø, Norway

ARTICLE INFO

Handling Editor: Dr. Jose Luis Domingo

Keywords:
Co-culture
Hepatocytes
Kidney cells
3D
Atlantic salmon
Glyphosate

ABSTRACT

A novel 3D Atlantic salmon co-culture model was developed using primary hepatocytes and kidney epithelial cells isolated from the same fish. Mono and co-cultures of primary hepatocytes and kidney epithelial cells were exposed for 48 h to glyphosate (5, 50 and 500 μM). For comparison, cells were also exposed to chlorpyrifos, benzo(a)pyrene and cadmium. Cell staining, cell viability assessments, RT-qPCR and global metabolomic profiling were used to examine the toxicological effects on liver and renal function and to compare responses in 3D and 2D cultures. The 3D hepatocyte cell culture was considered superior to the 2D culture due to the ATP binding cassette subfamily B member 1 (*Abcb1)* response and was thus used further in co-culture with kidney cells. Metabolomic analysis of co-cultured cells showed that glyphosate exposure (500 μM) altered lipid metabolism in both hepatocytes and kidney cells. Elevated levels of several types of PUFAs and long-chain fatty acids were observed in exposed hepatocytes, owing to increased uptake and phospholipid remodelling. Glyphosate suppressed the expression of estrogen receptor 1 (*Esr1*) and vitellogenin (*Vtg*) and altered histidine metabolism in exposed hepatocytes. Increased levels of cholesterol and downregulation of clusterin (*Clu)* suggest that glyphosate treatment affected membrane stability in Atlantic salmon kidney cells. This study demonstrates the usefulness of applying 3D co-culture models in risk assessment.

1. Introduction

Primary cell cultures are valuable tools in risk assessment of contaminants, since the primary cells retain the basic characteristic of the tissue from which they originate and thus respond in a tissue-like fashion (Segner and Braunbeck, 2003; Søfteland et al., 2011). By applying *in vitro* assays, contaminant toxicity can be analysed faster and more cost-efficient than with *in vivo* models (Stegeman and Hahn, 1994; Sung et al., 2013). The downside of two-dimensional (2D) mono cell cultures is that they may not account for cell-to-cell transfer or inter-tissue distribution of contaminants (Fent, 2001; Bhogal et al., 2005) as well as lacking the essential interplay with the endocrine and the immune systems (Edling et al., 2009) and other organs which occur *in vivo*. The development of 2D co-culture models increase the sensitivity of the system by including communication between different cell types (Edling et al., 2009; Holen et al., 2014) and by recreating intracellular networks *in vitro* (Bhogal et al., 2005). The development of Atlantic salmon primary co-cultures from hepatocytes and head kidney cells improved the responsivnes of the cells compared to both liver and head kidney monocultures (Holen et al., 2014). To replace *in vitro* models currently in use in toxicology research, new models must be further refined. The sensitivity and relevance of *in vitro* cell models can be improved even more by using three-dimensional (3D) co-cultures. Due to their *in vivo*-like responses, 3D co-cultures have become more commonly used in pharmaceutical and chemical research (Huh et al., 2011). Culturing cells isolated from vital organs with 3D scaffolds, creates cell-culture microenviroments that both supports tissue differentiation and recapitulate the tissue-tissue interfaces and microenvironments of living organs (Huh et al., 2011; Breslin and Lorraine O'Driscoll, 2013).

One or more organs are involved in metabolisation of contaminants. In certain cases, contaminants can be bioactivated and metabolites can travel to and cause toxic effects in remote organs (Li and Chiang, 2009). Even if the liver is the primary target organ for many contaminants, the kidney is also a frequent target organ for contaminants. Kidney epithelial cells, which have proximal tubule function and is the most common site of contaminant injury (Taub, 2005), are often applied in toxicity assessments. These cells predominantly express all cytochrome P450 (CYP) and b-lyase enzymes in the kidney (Schnellmann, 2008). A method for isolation of primary kidney epithelial have been develop for

* Corresponding author.
E-mail address: Liv.Softeland@hi.no (L. Søfteland).

https://doi.org/10.1016/j.fct.2022.113012
Received 20 October 2021; Received in revised form 5 April 2022; Accepted 9 April 2022
Available online 14 April 2022

Abbreviations

ABCB1	ATP binding cassette subfamily B member 1
ALPL	Alkaline phosphatase liver/bone/kidney isozyme
ANOVA	Analysis of variance
CPT2	Carnitine o-palmitoyltransferase 2
CYP	Cytochrome P450
CYP**1A**1	Cytochrome P450 family 1 subfamily A member 1
CI	Cell index
CLU	Clusterin
cDNA	Complementary DNA
CAR	Constitutive androstane receptor
CT	Crossing point
CD324	E-cadherin
EPSP	5-enolpyruvylshikimate-3-phosphate synthase
DHA	Docosahexaenoate
DPA	Docosapentaenoate
EPA	Eicosapentaenoate
EF1AB	Elongation factor 1 AB
ESI	Electrospray ionization
ENO1	Enolase 1
ESR1	Estrogen receptor 1
EDTA	Ethylenediaminetetraacetic acid
FDR	False discovery rate
FABP3	Fatty acid binding protein 3
FC	Fold-change
FT-ICR	Fourier transform ion cyclotron resonance
GC-MS	Gas chromatography–mass spectrometry
GMO	Genetically modified organisms
HO	Heme oxygenase 1
HMDB	Human metabolome database
H_2O_2	Hydrogen peroxide
IPA	Ingenuity pathway analysis
CD29	Integrin beta-1
HAVCR1	Kidney injury molecule 1
L-15	Leibovitz
LIT	Linear ion-trap
LC/MS/MS	Liquid chromatography with tandem mass spectrometry
LPLAT	Lysophospholipid acyltransferase
MRL	Maximum residue level
MNE	Mean normalized expression
MTT	3-[4,5-domethylthiazol-2-yl]-2,5-diphenyl tetrazolium bromide
NTC	No-template control
NAC	No-amplification control
NCI	Normalized CI
PPARα	Peroxisome proliferator-activated receptor α
PBS	Phosphate buffered saline
PLA_2	Phospholipase A
PUFA	Polyunsaturated fatty acid
RXR	Retinoid X receptor
RT-qPCR	Reverse transcription quantitative real-time PCR
ROS	Reactive oxygen species
RIN	RNA integrity number
RT	Reverse transcription
SREBF2	Sterol regulatory element binding transcription factor 2
3D	Three-dimensional
2D	Two-dimensional
UBA52	Ubiquitin A-52 residue ribosomal protein fusion product 1
VTG	Vitellogenin

flounder (Bols and Lee, 1991), however, an equivalent method for Atlantic salmon has not been established. In previous exposure studies with Atlantic salmon hepatocytes, we have shown low inducibility of *cyp1a* in monocultures (Olsvik et al., 2017; Olsvik and Søfteland, 2020). However, using co-culture of primary kidney epithelial cells and hepatocytes showed that monooxygenase activity was systematically higher in co-cultures than in conventional hepatocyte cultures (Donato et al., 1994).

Increased use of plant feed ingredients introduces a new contaminant profile that has not previously been associated with farming of salmonids. Glyphosate is a broad-spectrum herbicide and [N-(phosphonomethyl) glycine] is the active ingredient of the end-product Roundup. This widely utilized pesticide is used in large quantities all over the world on GMO (genetically modified organisms) crops and non-GMO crops (Benbrook, 2016) and was recently detected in commercial salmon feed (Ørnsrud et al., 2020). The glyphosate detected in Norwegian salmon feed originates from non-GMO sources since GMO feed ingredients is not allowed in Norway (Norwegian food safety authority, 2022). Glyphosate was for the first time included in the Norwegian feed surveillance in 2016. In 2020, 36 of 40 salmon feed (mean 0.07 mg/kg, or 0.41 μM), 7 of 19 vegetable feed ingredients (mean 0.33 mg/kg, or 1.95 μM) and three of four insect meal samples (mean 0.03 mg/kg, or 0.17 μM) analysed contained glyphosate (Sele et al., 2021). Today a Maximum residue level (MRL) for glyphosate is still lacking for fish feed and feed ingredients' (Ørnsrud et al., 2020). Increasing number of glyphosate toxicity studies suggest that glyphosate may constitute a risk for farmed Atlantic salmon since renal and hepatic impairment have been detected in exposed fish (Langiano and Martinez, 2008; Shiogiri et al., 2012). Further, disturbed steroidogenic biosynthesis pathway, oxidative stress and reproductive toxicity have been linked to glyphosate exposure in zebrafish (*Danio rerio*) (Webster et al., 2014). In vertebrates, cytotoxicity and genotoxic effects have been detected after glyphosate exposure (Gill et al., 2018). The physiological implications and possible health effects posed by glyphosate to Atlantic salmon are not fully known.

The aim of the study was to develop a method to isolate primary kidney epithelial cells and to use these 2D kidney epithelial cells in a co-culture with 3D primary hepatocytes from Atlantic salmon. To validate the usefulness of the 3D co-culture model, the toxicological effects of glyphosate was assessed with cell staining, cell viability and oxidative stress assays in addition to reverse transcription quantitative real-time PCR (RT-qPCR) evaluation and metabolomics profiling. In addition, three toxicants with known *in vitro* toxicity in Atlantic salmon; chlorpyrifos, benzo(a)pyrene and cadmium, were included to obtain a more thorough evaluation of the novel primary co-culture model.

2. Materials and methods

2.1. Chemicals

Benzo(a)pyrene (96% pure), chlorpyrifos (O,O-diethyl-O-3,5,6-trichlor-2-pyridyl phosphorothioate PESTANAL®, analytical standard), glyphosate (PESTANAL®, analytical standard) and dimethyl sulfoxide stock solution were all purchased from Sigma-Aldrich (Oslo, Norway) and cadmium ($CdCl_2$) was purchased from Merck (Darmstadt, Germany).

2.2. Isolation of primary cultures of hepatocytes

Hepatocytes were isolated from six male Atlantic salmon (415–715 g) with a two-step perfusion method previously described in Søfteland et al. (2009). Fish handling was approved by the Norwegian Animal Research Authority (FOTS ID, 19351). The final cell pellet was resuspended in L-15 medium (without phenol red) containing 10% fetal

bovine serum (Sigma Aldrich), 1% glutamax (Invitrogen, Norway) and 1% penicillin-streptomycin-amphotericin (10000 units/ml potassium penicillin, 10000 μg/ml streptomycin sulphate and 25 μg/ml amphotericin B) (Lonzo, Medprobe, Oslo, Norway). The Trypan Blue exclusion method, performed in accordance with the manufacturer's protocol (Lonzo, Medprobe, Oslo, Norway), was used to determine cell viability. The different cell suspensions used in this study had hepatocyte cell viability between 93 and 97%. The hepatocytes were plated on 2 μg/cm^2 laminin (Sigma-Aldrich, Oslo, Norway) coated 3D Alvetex Scaffolds (200 μm cross-linked polystyrene membranes, 42 μm mean void size, Reprocell, Glasgow, United Kingdom) in 12 well culture plates (Falcon, Corning, VWR, Bergen, Norway) and 2 μg/cm^2 laminin (Sigma-Aldrich) coated 2D 12 well culture plates. The following cell concentrations were used; 2.9 × 10^6 cells per well in 12-well plates (2D and 3D cells in 2 and 2.5 ml complete L-15 (Leibovitz) medium respectively), 0.2 × 10^6 cells per well in xCELLigence 96-well plates (in 0.150 ml complete L-15 medium), 3D 96-well plates with Alvetex Scaffolds (in 0.150 ml complete L-15 medium) and 2D 96-well plates in 0.2 ml complete L-15 medium.

2.3. Isolation of primary cultures of kidney cells

2.3.1. Isolation of primary cultures of kidney cells using Percoll density-gradients

The kidney cell isolation method is based on the Atlantic salmon primary hepatocyte isolation method described by Søfteland et al. (2009) and the protocol of Lash (1996) for isolation of primary rat kidney epithelial renal proximal tubular and distal tubular cells (Fischer 344 rats).

After the isolation of the primary hepatocytes, the intestine, swim bladder and the exterior kidney membrane were removed. A spoon was used to remove the kidney from the fish and transferred to a petri dish filled with collagenase VIII (1 mg/ml, same solution as used for the hepatocyte isolation) (Sigma–Aldrich). The kidney was cut into small pieces with a scalpel and transferred to a bottle containing 100 ml collagenase VIII (1 mg/ml). The kidney cells were gently shaken for 7 min at room temperature. Subsequently, the cell suspensions were filtered through 200 and 100 μm nylon gauze cell filters and divided into four 50 ml centrifugations tubes. 25 ml perfusion buffer with EDTA (25.3 mM ethylenediaminetetraacetic acid, Sigma–Aldrich), same buffer as used in the isolation of the hepatocytes, was added to each tube. The cells were collected by centrifugation (150×*g* for 5 min, 4 °C). The supernatant was decanted, and the cell pellet resuspended in 15 ml perfusion buffer with EDTA. A Percoll density-gradient centrifugation was used for purification of the kidney cells. Four 50 ml centrifugation tubes were prepared (1.016 g/ml, 1.047 g/ml, 1.057 g/ml, 1.076 g/ml and 1.120 g/ml, 5 ml per gradient) and 15 ml cell suspension were carefully applied on the top of each gradient. The cells were collected by centrifugation (800×*g* for 30 min, 4 °C). Cells were collected from the gradients: 1.016 g/ml, 1.047 g/ml, 1.057 g/ml, and 1.076 g/ml. Cells were resuspended in 40 ml of perfusion buffer with EDTA and cells were collected by centrifugation (500×*g* for 5 min, 4 °C). The cells were resuspended a second time in 40 ml perfusion buffer with EDTA and collected by centrifugation (150×*g* for 5 min, 4 °C). The supernatant was decanted, and the cell pellet resuspended in complete L-15 medium. The viability of the kidney cells was determined with the Trypan Blue exclusion method and kidney cells cell viability varied between 87 and 99%. 0.5 × 10^6 cells (in 0.5 ml complete L-15 medium) were plated on laminin (2 μg/cm^2; Sigma–Aldrich) coated 12 well cell inserts (Falcon, Corning, VWR) and 0.1 × 10^6 cells (in 0.05 ml complete L-15 medium) were plated on laminin (2 μg/cm^2; Sigma–Aldrich) coated 96 well cell inserts (ACEA Biosciences, Inc., Aarhus, Denmark) for the xCELLigence and the 3D 96 well plates. The primary hepatocyte and kidney cells were kept at 10 °C in a sterile incubator without additional O_2/CO_2 (Sanyo, CFC FREE, Etten Leur, Netherland).

2.3.2. Isolation of kidney cells using Ficoll density-gradients

To compare cell yield, kidney cells were isolated as described in 2.3.1, however a Ficoll density-gradient centrifugation was performed instead of a Percoll density-gradient centrifugation to purify the kidney cells. The kidney cell purification method was performed according to the Ficoll manufacture's protocol (GE Healthcare, Oslo, Norway).

2.4. Cell staining

24 h after isolation the kidney cells were stained with hematoxylin and neutral red.

2.4.1. Hematoxylin cell staining

Hematoxylin has a blue-purple color and the nucleic acids are stained by a complex reaction which leads to that the nuclei is stained blue (Fischer et al., 2008). Unexposed primary kidney cells were plated onto 8-well chamber slides (Lab-tek, Nunc, Rochester, USA). The hematoxylin staining was performed according to the Steatosis Colorimetric Assay Kit (Cayman Chemical, Ann Arbor, USA) manufacturer's protocol. The stained cells were sealed onto the slides with a coverslip and one drop of Gel Mount Aqueous Mounting Medium (Sigma–Aldrich) and evaluated under Bright-field using an inverted microscope (Axiovert 40 CFL with an Axiocam ICc3 camera and Axiovision Rel. 4.8 microscopy software, Zeizz, Oslo, Norway) under 40x magnification.

2.4.2. Neutral red cell staining

The neutral red cell staining gives a quantitative assessment of cells viability. The method is based on that the neutral red dye is incorporated into lysosomes of viable cells (Repetto et al., 2008). Unexposed 3D primary hepatocytes on Alvetex Scaffold disc and 2D primary kidney cells on well inserts were washed with phosphate buffered saline (PBS) and stained for 5 min at room temperature with neutral red 0.33% solution (Sigma–Aldrich), diluted 1:1 with PBS, according to Alvetex Scaffold's protocol (Reprocell). The cultures were washed 3 times with 4 ml PBS for 5 min on a platform shaker (100 rpm). After removing the last PBS wash, Alvetex Scaffold discs and 2D inserts were separated from their holders, placed on microscope glass slides with 150 μL PBS and glass coverslips. The stained cells were photographed with brightfield illumination using an inverted microscope (Axiovert 40 CFL with an Axiocam ICc3 camera and Axiovision Rel. 4.8 microscopy software, Zeizz) under 10x and 40x magnification.

2.5. Chemical exposure

The primary cells were cultured for 36–40 h prior to chemical exposure with one change of medium (containing 10% FBS) after 18–20 h. The cells were exposed for 48 h to single contaminants to establish dose-response curves for glyphosate (5, 50 and 500 μM, liver and kidney cells from six fish, N = 6), chlorpyrifos (1 and 10 μM, N = 3), benzo(a)pyrene (0.1 and 1 μM, N = 3) and cadmium (10 μM, N = 3). The concentrations used of chlorpyrifos, benzo(a)pyrene and cadmium were selected based on earlier *in vitro* toxicity assessments (Søfteland et al., 2014: Søfteland et al., 2010; Olsvik et al., 2016). The 2D hepatocytes and 3D hepatocytes co-cultured with 2D kidney cells were isolated from three or six fish, and the hepatocytes co-cultured with 2D kidney cells were isolated from the same fish. The chemical exposure medium was substituted with new medium after 18–20 h. The toxicological cellular response was analysed using cytotoxicity, ROS-Glo™ H_2O_2 Assay, qPCR and metabolomics.

2.6. Cytotoxicity testing of chemicals

2.6.1. xCELLigence

For the cytotoxicity assessment of contaminants, real time impedance data obtained by the xCELLigence systems (ACEA Biosciences, AH diagnostics AS, Oslo, Norway) was used. The xCELLigence system

Table 1
PCR primers, GenBank accession numbers, amplicon sizes and PCR efficiencies.

Gene	Accession no.	Forward primer (5′–3′)	Reverse primer (5′–3′)	Product size (bp)	Efficiency
Cyp1a	AF364076	TGGAGATCTTCCGGCACTCT	CAGGTGTCCTTGGGAATGGA	101	2.0/2.1
Abcb1	AY863423	AGCAGTGGCTGTGGGAAGAG	CCCTCAGCCAATGGATGTTC	121	2.2
Abcc1	EG908489	TGGCAGTCTGAGGATGAACCT	CGGCTGGTTGCTGACAAACT	106	2.0
Abcc3	GQ888533	TCTGGAACTGTCCCACCTCAA	CTGGCCCACACTGAGGTTCT	97	2.0
Srebf2	XM_014203734	CTGTCTGGCAACTGGCTCAA	CTCCCCATTGCTGCTGCTT	105	2.1
Sc5d	XM_029690808	CCCTCTGCACAAGGTGCTTT	CCCGTTGACCACCTCCTGTA	115	1.9
Fabp3	BT125322	CCGCCGACGACAGAAAAA	TTTTGCACAAGGTTGCCATTT	61	1.9
Cpt2	BG934647	TGCTCAGCTAGCGTTCCATATG	AGTGCTGCAGGACTCGTATGTG	49	2.2
Eno1	NM_001139894	ATCCAGGTGGTGGGTGATGA	CGGAGCCGATCTGGTTGA	112	2.0
Ho	BG936101	AGCAGATTAAAGCTGTAACCAAGGA	GCCAGCATCAGCTCAGTGTTC	64	1.8/1.9/2.0
Clu	NM_001173637	ATGATGGACATGGCCTGGAA	CCGGAAGGCTTTGTCACAAC	128	2.0/1.9
Havcr1	XM_014136749	ACAACGTCGGAGAGGGAGACT	TGCGTCAGGTCGTTGAACAG	76	1.9/2.0
Esr1	XM_014205564	GGTCTCCCCAGCCAGTCATA	TGGAGGTGATGCAGAGCTTCT	112	2.1
Vtg	C065R146	GACTTCGCCATCAGCCTTTC	GCCACGGTCTCCAAGAAGTCT	110	2.1
Cd324	XM_014175509	CCGTAATGACATCGCTCCAA	TCGTTGTCAGCTGCCTTCAG	111	2.0
Cd29	XM_014180509	CTCGTTGGTGCTGCACTCA	ACAACGGCAACGGGACATAT	86	2.1
Alpl	XM_014133549	GGCCCAGCGTACTTTGAAGA	CTGCCGTCACTGTGGGAAT	113	2.0
Ef1ab	AF321836	TGCCCCTCCAGGATGTCTAC	CACGGCCCACAGGTACT	59	1.9/2.0
Uba52	GO050814	TCAAGGCCAAGATCCAGGAT	CGCAGCACAAGATGCAGAGT	139	1.8/1.9
β-actin	BG933897	CCAAAGCCAACAGGGAGAA	AGGGACAACACTGCCTGGAT	92	1.9/2.0

quantifies electrical impedance across electrodes in 96-well cell culture E-Plates. The impedance measurement gives quantitative information about the cells' health status including morphology, cell number and viability and is indicated with the parameter Cell index (CI) or the normalized CI (NCI). The xCELLigence instrument was used to establish dose-response relationship for the contaminants in exposed 2D primary hepatocytes co-cultured with 2D kidney cells. The real time cell monitoring was conducted at 10 °C in an incubator without additional O_2/CO_2 (Sanyo, CFC FREE, Etten Leur, Netherland), using the RTCA single plate xCELLigence platform. The data was collected according to Søfteland et al. (2014). Briefly, the data was collected with intervals of 2 min after contaminant exposure for 12 h, and then every 15 min for 120 h. The last time point before compound exposure was used for the normalization, allowing a more precise comparison of the effect of the different contaminant concentrations tested. The CI values presented here were calculated from three to six replicate values. Determination of cytotoxic effects were done according to the International standardised test for *in vitro* cytotoxicity, ISO 10993-5:2009 (ISO, 2009). Contaminants will be deemed cytotoxic when cells viability exceeds 30% reduction compared to the control. Primary hepatocytes isolated from three or six fish were used for the xCELLigence analysis (N = 3 and N = 6).

2.6.2. MTT

A MTT-based (3-[4,5-domethylthiazol-2-yl]-2,5-diphenyl tetrazolium bromide) *in vitro* toxicity assay was performed in accordance with the manufacturer's protocols (Sigma–Aldrich). The MTT test is based on spectrophotometric determination of cell number as a function of mitochondrial activity in living cells. The MTT solution was dissolved in PBS. The absorbance was measured after 4 h incubation at 570 nm using VICTOR X5 Multilabel Plate Reader (PerkinElmer, Oslo, Norway). 2D primary hepatocytes and 3D hepatocytes co-cultured with kidney cells and 2 D kidney cells isolated from three or six fish were used for the MTT analysis (N = 3 and N = 6).

2.7. ROS-Glo™ H_2O_2 Assay

The ROS-Glo™ H_2O_2 Assay is a sensitive bioluminescent assay that assess oxidative stress or reactive oxygen species (ROS), by evaluating the level of hydrogen peroxide (H_2O_2) in the cell cultures. Samples are incubated with a luciferin substrate that reacts directly with H_2O_2 to produce a luciferin precursor. The precursor converts to luciferin and provides Ultra-Glo™ Recombinant Luciferase when ROS-Glo™ Detection Solution are added and the level of H_2O_2 in samples are proportional to the light signal produced (Promega, Oslo Norway). The ROS-Glo™ H_2O_2 Assay was performed according to the manufacturer's procedures and quantified using the VICTOR X5 Multilabel Plate Reader (PerkinElmer, Oslo, Norway). 2D hepatocytes co-cultured with 2D kidney cells from three or six fish were used for the analysis (n = 3 and n = 6).

2.8. RNA extraction and reverse transcription quantitative real-time PCR

2.8.1. RNA extraction

The RNeasy Plus mini kit (Qiagen, Crawley, UK) was used to extract total RNA from the primary kidney cells and 2D primary hepatocytes according to the manufacturer's protocol. The RNeasy Plus mini kit (Qiagen, Crawley, UK) was also used to extract total RNA from the 3D hepatocytes, however the RNA extraction was performed according to Alvetex Scaffold's protocol (Reprocell). In short cells were washed with PBS and lysed by adding 600 μl Qiagen RNeasy Plus mini kit lysis buffer RLT per well and placed for 10 min on a rotating platform (100 rpm) at room temperature. The lysate was homogenized 10 times with a 20-gauge needle. 600 μl 70% ethanol was added to the homogenized lysate. A pipette was used to mix the sample 10 times before transfer to a collection tube and stored at −80 °C. Samples were thawed and transferred to RNeasy® spin column. A DNase digestion on-column was performed before finalizing the RNeasy Plus mini kit protocol. RNA was eluted in 30 μl RNase-free MilliQ H_2O. The RNA quantity and quality were assessed with the NanoDrop® ND-1000 UV–Vis Spectrophotometer (NanoDrop Technologies, Wilmington, DE, USA) and the Agilent 2100 Bioanalyzer (Agilent Technologies, Palo Alto, CA, USA) pursuant to the manufacturer's instructions. The integrity of the RNA was evaluated with the RNA 6000 Nano LabChip® kit (Agilent Technologies). The samples used in this experiment had 260/280 nm absorbance ratios and a 260/230 nm ratios above 2 and RNA integrity number (RIN) values above 9, which indicate pure RNA and intact samples (Schroeder et al., 2006).

2.8.2. Whole transcriptome amplification

Due to weak attachment of the kidney cells to the cell plates and lack of a commercial 3D scaffold that works at 10 °C, a QuantiTect Whole Transciptome kit (Qiagen, Crawley, UK) was used to amplify RNA from the primary kidney cells and was performed according to the manufacturer's protocol.

2.8.3. Reverse transcription quantitative real-time PCR

The transcriptional levels of selected target genes were quantified with a two-step reverse transcription quantitative real-time PCR (RT-

qPCR) protocol. A serial dilution curve of total RNA with six points in triplicates between 1000 and 31 ng were made for PCR efficiency calculations. 500 ng of total RNA was added to the reaction for each sample, and reverse transcription (RT) reactions were run in duplicates using 96-well reaction plates. No-template control (ntc) and no-amplification control (nac) reactions were run for quality assessment for every gene assay. The 50 μl RT reactions were performed at 48 °C for 60 min utilizing a GeneAmp PCR 9700 thermocycler (Applied Biosystems, Foster City, CA, USA). Individual RT reactions contained 1X TaqMan RT buffer (10X), 5.5 mM $MgCl_2$, 500 mM dNTP (of each), oligo dT primers (2.5 μM), 0.4 U/μl RNase inhibitor and 1.67 U/μl Multiscribe Reverse Transcriptase (Applied Biosystems) and RNase-free water.

For every gene analysed, real-time qPCR was run in 10 μl reactions on a LightCycler® 480 Real-Time PCR System (Roche Applied Sciences, Basel, Switzerland) containing 2.0 μl complementary DNA (cDNA, diluted twofold). The real-time qPCR was carried out in two 384-well reaction plates using SYBR Green Master Mix (LightCycler 480 SYBR Green master mix kit, Roche Applied Sciences, Basel, Switzerland) containing gene-specific primers and FastStart DNA polymerase. PCR runs were performed with a 5 min activation and denaturing step at 95 °C, followed by 45 cycles with each cycle consisting of a 10 s denaturing step at 95 °C, a 10 s annealing step (60 °C) and finally a 10 s extension step at 72 °C. The primer pairs had an annealing temperature of 60 °C. See Table 1 for primer sequences, amplicon sizes and GenBank accession numbers. Final primer concentrations of 500 nM were used. For confirmation of amplification of gene-specific products, a melting curve analysis was carried out and the second derivative maximum method (Tellmann, 2006) was used to determine crossing point (CT) values using the Lightcycler 480 Software. To calculate the mean normalized expression (MNE) of the target genes, the geNorm VBA applet for Microsoft Excel version 3.4 was used to calculate a normalization factor based on three reference genes. By using gene-specific efficiencies calculated from the standard curves, the CT values are converted into quantities (Vandesompele et al., 2002). Elongation factor 1 AB (*ef1ab*), ubiquitin A-52 residue ribosomal protein fusion product 1 (*uba52*) and *β-actin* were the selected reference genes for this experiment. The reference genes were stable with gene expression stability (M) values of 0.309. 2D and 3D hepatocytes co-cultured with 2D kidney cells from three or six fish were used for the analysis (N = 3 and N = 6).

2.9. Metabolomics

2.9.1. Sample preparation

500 μl cell medium was taken from each well to make a pooled sample for control and 500 μM glyphosate before the cells were harvested. Retrieval of cells from Alvetex® Scaffold for the metabolomics analysis were performed according to Alvetex Scaffold's protocol (Reprocell). In short, the well inserts with the kidney cells were transferred to new exposure plate with 12 wells. The kidney cells and 3D hepatocytes were washed with PBS. The hepatocytes were incubated with 1.5 ml 0.25% trypsin for 15 min on a rotating platform (100 rpm) at room temperature. The kidney cells were incubated for 3 min with 1.5 ml 0.25% trypsin at room temperature. 2 ml complete medium were used to stop the trypsin reaction. The cell suspension was transferred to centrifugation tubes and centrifuged at 1000×*g* for 5 min at 4 °C. The supernatant was discharged, the cells were dissolved in 2 ml PBS and wasted a second time at 1000×*g* for 5 min at 4 °C. Three 12-wells with cells were pooled. Cells and medium were flash frozen and stored at −80 °C.

2.9.2. Metabolomic screening

Global metabolite profiles were determined in 12 hepatocytes (3D) and in 12 kidney (2D) samples, i.e. in 6 controls and 6 exposed to 500 μM glyphosate per cell type. Sample extraction and metabolite analysis were performed according to Metabolon's standard solvent extraction method and as previously described by Olsvik et al. (2015). In short, the sample extracts were divided into two equal parts for gas chromatography/mass spectrometry (GC/MS) and liquid chromatography with tandem mass spectrometry (LC/MS/MS) analysis. The LC/MS platform was based on a Waters ACQUITY UPLC and a Thermo-Finnigan LTQ mass spectrometer, which consisted of an electrospray ionization (ESI) source and linear ion-trap (LIT) mass analyzer. The GC/MS samples were analysed on a Thermo-Finnigan Trace DSQ fast-scanning single--quadrupole mass spectrometer using electron impact ionization. Accurate mass determination and MS/MS fragmentation (LC/MS/MS) was based on Waters ACQUITY UPLC and a Thermo-Finnigan LTQ-FT mass spectrometer, which had a linear ion-trap (LIT) front end and a fourier transform ion cyclotron resonance (FT-ICR) mass spectrometer backend. An accurate mass measurement could be performed on parent ion as well as fragments ions with counts greater than 2 million. Mass error was typically less than 5 ppm. Instrument variability was 4% for internal standards and total process variability for endogenous metabolites was 12%. Identification of known chemical entities was based on comparison to metabolomic library entries of purified standards. The metabolomic screening was conducted by employees at Metabolon. Inc. (Durham, NC, USA).

2.10. Statistics

The GraphPad Prism 8.3.0 software (GraphPad Software. Inc., San Diego. CA. USA) was used for statistical analyses of the MTT, xCELLigence, ROS-Glo™ H_2O_2 Assays and gene expression data. The Brown-Forsythe and Bartlett's tests were used to check for normality and the data were log transformed prior to the statistical analysis when required. The ROUT method was applied to detect outliers. This method uses the false discovery rate (FDR) and predicts that 1% are false outliers. One-way analysis of variance (ANOVA) repeated measurement and two-way ANOVA repeated measurement with Dunnett's or Tukey's post-test and two-tailed T-test analysis were used to compare exposed cells with the controls (significance level of $P < 0.05$).

Pathways enrichment analysis was done by annotation with the KEGG database (blastx $E10^{-5}$) to calculate differential metabolite expression. Following normalization to dsDNA concentration, log transformation, Welch's two-sample t-tests were used to identify biochemicals/metabolites that differed significantly between the experimental groups ($P < 0.05$). Missing values from the metabolite screening were assumed to be below the limits of detection and these values were imputed with the compound minimum (minimum value imputation). Correction for multiple testing was done with FDR using q-values (P-adj) (Benjamini and Hochberg, 1995). Statistical analyses of the log-transformed data were performed with the program "R" (The Comprehensive R Archive Network). Due to limited sample amount, only DNA levels were quantified for kidney cells. Because protein and DNA levels measured in hepatocytes showed very good correlation ($r^2 = 0.91$), and similar trends were observed between protein- and DNA-normalized datasets, the metabolite data were normalized to DNA for both liver and kidney cells.

Functional pathway analyses were generated through the use of QIAGEN's Ingenuity pathway analysis (IPA®, QIAGEN Redwood City, www.qiagen.com/ingenuity) and were based on metabolite and RT-qPCR data. IPA used PubChem (a database on biological active molecules) and Human metabolome database (HMDB) and Human gene symbols (Hugo/HGNC ID, Entrez Gene ID/KEGG) mapped entities.

3. Results

3.1. 2D kidney cells and 3D hepatocytes

To verify that the cell separation techniques isolated kidney epithelial cells, cell yield from different Percoll density gradients (1.016 g/ml, 1.047, 1.057, 1.076, 1.120) and a Ficoll gradient were analysed with specific qPCR markers for three kidney epithelial cells. Alkaline

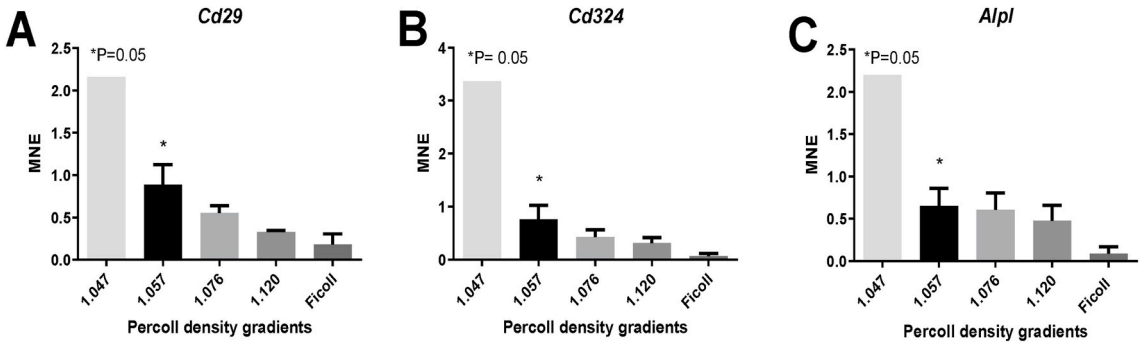

Fig. 1. Transcriptional markers for kidney epithelial cells expressed in different Percoll and Ficoll density gradients (N = 1 and 4). A) *Cd29*, B) *Cd324* and C) *Alpl* were used to verify that the cell separation techniques isolated kidney epithelial cells. The analyses showed significant difference between the Ficoll and the Percoll gradient indicated with an asterisk (one-way ANOVA, Dunnett's post-test, mean ± SEM * P = 0.05).

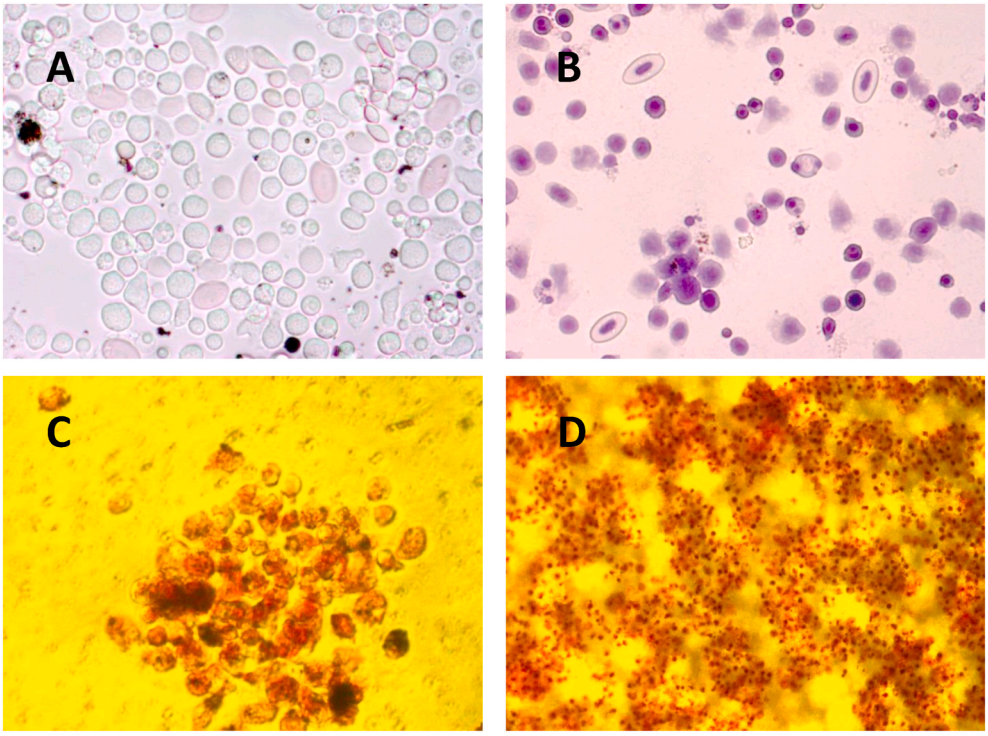

Fig. 2. A) Bright-field light microscopy of freshly isolated 2D kidney cells (40X), B) 2D hematoxylin stained renal proximal tubular and distal tubular cells (40X), C) neutral red stained 2D kidney cells on a Falcon cell insert (0.4 pore size, 40X) and D) 3D primary hepatocytes on an Alvetex scaffold (10X). Cells were isolated from six male Atlantic salmon (N = 6). (For interpretation of the references to color in this figure legend, the reader is referred to the Web version of this article.)

phosphatase liver/bone/kidney isozyme (*Alpl*), integrin beta-1 (*Cd29*), E-cadherin (*Cd324*) were all higher expressed in the Percoll gradients than the Ficoll gradient though the levels were only significantly higher in the 1.057 Percoll gradient compared to the Ficoll gradient (Fig. 1A and B and C). Cells from the Percoll gradients 1.016 g/ml, 1.047 g/ml, 1.057 g/ml and 1.076 g/m were combined, and the freshly isolated 2D kidney cells (Fig. 2A) and cells stained with hematoxylin (Fig. 2B) and neutral red (Fig. 2C) were evaluated with a bright field light microscopy. The freshly isolated and the hematoxylin stained cells showed that the percoll gradient method is isolating mainly renal proximal tubular and distal tubular cells. In addition, the isolation method was providing viable cells, as visualised by neutral red staining of the 2D kidney cells (Fig. 2C). Fig. 2D shows viable neutral red stained 3D hepatocytes on Alvetex scaffold.

3.2. Cell viability and ROS-Glo™ H_2O_2 Assays

To evaluate the toxicological response of the 2D kidney cells, 2D and 3D hepatocytes, the cells were co-cultured and exposed to glyphosate (5, 50 and 500 μM), cadmium (10 μM), chlorpyrifos (1 and 10 μM) and benzo(a)pyrene (0.1 and 1 μM). The MTT assay, evaluating cells viability, did not show any significant changes between 2D hepatocytes and 3D hepatocytes co-cultured with 2D kidney cells compared to the control groups (Fig. 3A, C, E and G). None of the test substances induced any significant changes to xCELLigence-assessed cytotoxicity (data not shown). Chemical-exposed 2D hepatocytes co-cultured with 2D kidney cells were also evaluated for oxidative stress with the ROS-Glo™ H_2O_2 assay (Fig. 3B, D, F and H). ROS production was only significantly reduced in cells exposed to 0.1 μM benzo(a)pyrene compared to the control (Fig. 3H, one-way ANOVA Tukey post-test, P = 0.0298). In contrast to the MTT results for liver cells, kidney cells responded differently to glyphosate exposure depending on if they were cultivated

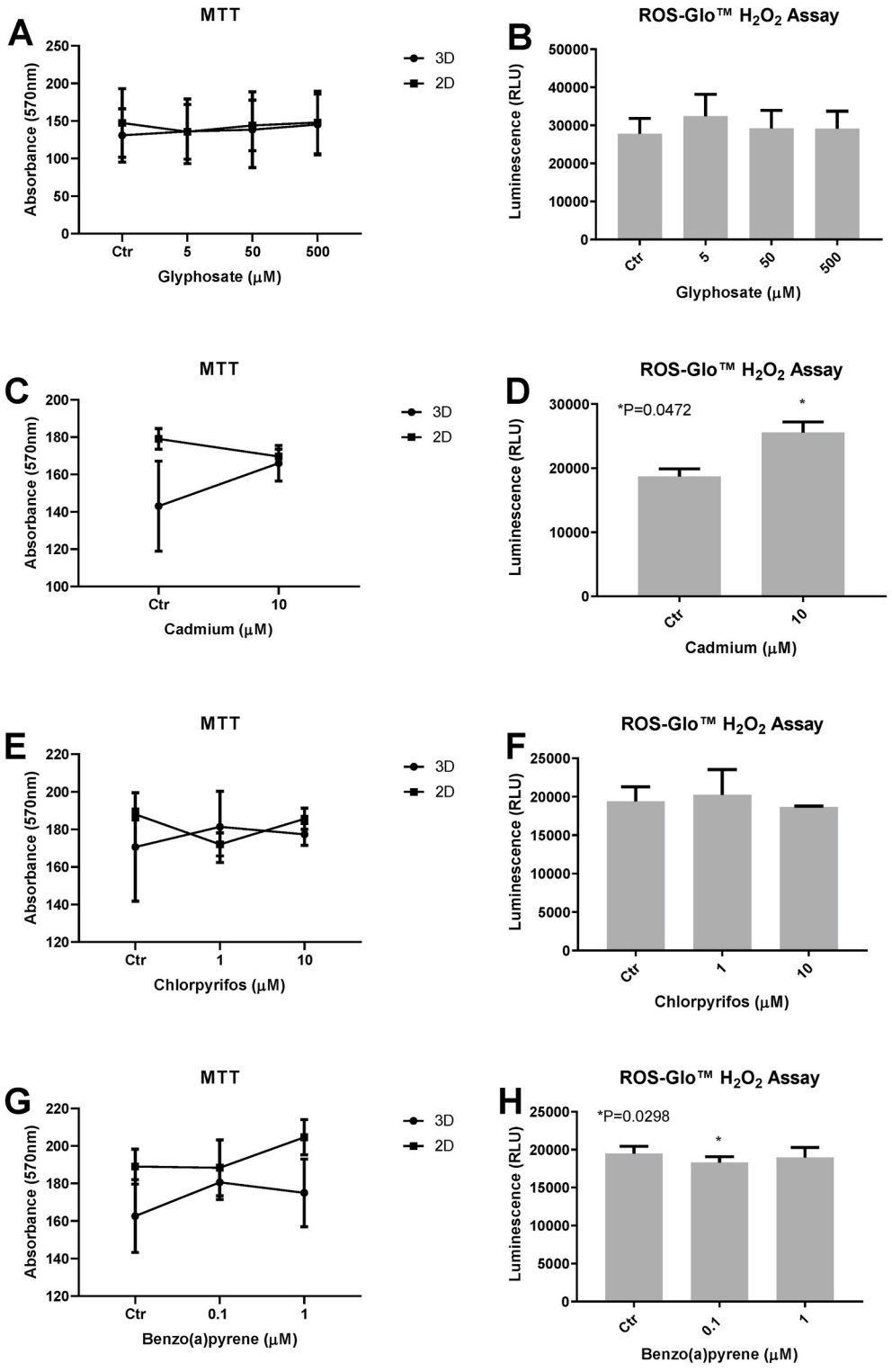

Fig. 3. MTT dose-response curves based on absorbance of 570 nm for 2D and 3D hepatocytes co-cultured with kidney cells and exposed to A) glyphosate (N = 6) C) cadmium (N = 3), E) chlorpyrifos (N = 3) and G) benzo(a)pyrene (N = 3). Ros-Glo™ H_2O_2 assessment of 2D hepatocyte - kidney co-cultures treated with B) glyphosate (N = 6), D) cadmium (N = 3), F) chlorpyrifos (N = 3) and H) benzo(a)pyrene (N = 3). Significant difference between control and exposed groups are indicated with an asterisk (one-way ANOVA with Dunnett's post-test and paired T-test, two-tailed, mean ± SEM, *P < 0.05).

with 2D or 3D hepatocytes. Cell viability was higher in 3D cultivated hepatocytes compared to 2D hepatocytes (Fig. 4 A, P = 0.0096, two-way ANOVA with Tukey post-test).

3.3. Transcriptional responses

3.3.1. Primary Atlantic salmon hepatocytes

Only four of twelve selected target genes significantly regulated compared to the control when 3D hepatocytes co-cultured with 2D kidney cells were treated with glyphosate (Fig. 5A-L). The estrogenic markers *Esr1* (estrogen receptor 1) and vitellogenin (*Vtg*) showed both a dose-dependent decreased expression and were significantly down-regulated in 500 μM (P = 0.0263) and 50 μM (P = 0.0210) and 500 μM (P = 0.0068) exposed hepatocytes, respectively (one-way ANOVA, repeated measurement with Dunnett's post-test). The expression of transporter *Abcb1* (ATP binding cassette subfamily B member 1) and enolase 1 (*Eno1*) were in contrast significantly upregulated in hepatocytes treated with the two highest glyphosate concentrations 500 μM (P

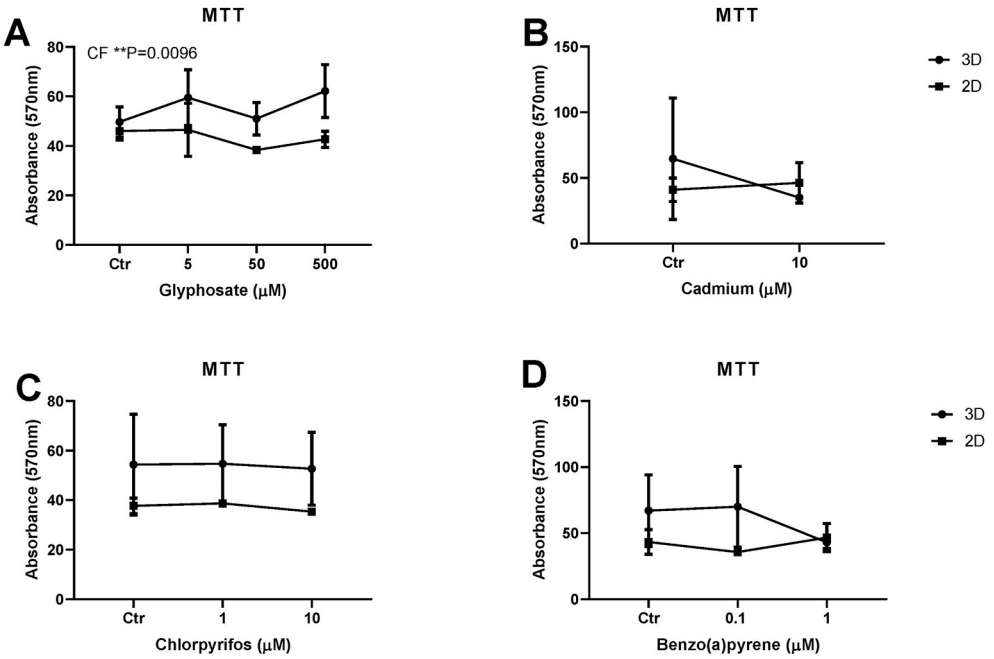

Fig. 4. MTT dose-response curves based on absorbance of 570 nm for 2D kidney cells co-cultured with 2D and 3D hepatocytes and exposed to A) glyphosate (N = 6) B) cadmium (N = 3), C) chlorpyrifos (N = 3) and D) benzo(a)pyrene (N = 3). Significant difference between control and exposed groups are indicated with an asterisk (two-way ANOVA with Tukey post-test, mean ± SEM, **P < 0.01). Cell system factor (CF).

= 0.0321 and P = 0.0017) and 50 μM glyphosate (P = 0.0239).

Similarly, only four of twelve target genes responded significantly in cadmium exposed 2D hepatocytes and 3D hepatocytes co-cultured with 2D kidney cells compared to control cells (Fig. 6A-L). In 2D hepatocytes treated with 10 μM cadmium, *Esr1* and *Vtg* were both downregulated (two-way ANOVA repeated measurement, Sidak's post-test, P = 0.0018 and P = 0.0004, respectively) and cadmium caused a similar down-regulation response in 3D hepatocytes (P = 0.0047 and P = 0.0004, respectively). Further, heme oxygenase 1 (*Ho*) was significantly upregulated in cadmium exposed 2D hepatocytes (P = 0.0066) and 3D hepatocytes (P = 0.0420). A similar response was observed after cadmium exposure with the transporter *Abcb1* (ATP binding cassette subfamily B member 1), however *Abcb1* was only upregulated in 3D exposed cells (P = 0.0203). In addition, the basal transcriptional levels of *Cyp1A1* (cytochrome P450 family 1 subfamily A member 1, P = 0.0010), *Fabp3* (fatty acid binding protein 3, P = 0.0166), *Srebf2* (sterol regulatory element binding transcription factor 2, P = 0.0256), *Abcb1* (P = 0.0006), *Abcc1* (P = 0.0128), *Abcc3* (P = 0.0019) and *Cpt2* (carnitine o-palmitoyltransferase 2, mitochondrial, P = 0.0385), in both control and cadmium exposed cells, were significantly higher in the 3D hepatocytes in contrast to the 2D hepatocytes.

In chlorpyrifos and benzo(a)pyrene exposed 2D hepatocytes and 3D hepatocytes co-cultured with 2D kidney cells, only *Cyp1a* was significantly upregulated (Fig. 7A–D). Both chemicals induced a dose-dependent increase in transcription. *Cyp1a* were significantly upregulated in 2D and 3D hepatocytes exposed to 0.1 and 1 μM benzo(a)pyrene (two-way ANOVA repeated measurement with Dunnett's post-test, P < 0.0001), however, *cyp1a* was only upregulated in cells treated with the highest chlorpyrifos concentration (3D P = 0.0136 and 2D P = 0.0019). Further, the chlorpyrifos exposure generated a relative higher *Cyp1a* and *Ho* basal transcription levels in the 3D control and exposed groups compared to the 2D hepatocyte groups (P = 0.0019 and P = 0.0125, respectively). The transcription levels of *Cyp1a* was also slightly higher in 3D hepatocytes exposed to benzo(a)pyrene (P = 0.0485).

3.3.2. Primary Atlantic salmon kidney cells

Three target genes related to kidney injury, *Ho*, clusterin (*Clu*) and kidney injury molecule 1 (*Havcr1*), were quantified in 2D kidney cells co-cultured with 3D hepatocytes treated with glyphosate, cadmium, chlorpyrifos and benzo(a)pyrene (Fig. 8A-L). Only *Clu* was significantly downregulated in cells exposed to 500 μM glyphosate compared to the 50 μM group (one-way ANOVA with Tukey post-test, P = 0.0410) and *Havcr1* was only significantly upregulated in cadmium treated cells compared to the controls (two-tailed T-test, P = 0.0064). *Havcr1* showed a trend to be significantly upregulated in 50 μM glyphosate exposed cells compared to the control (P < 0.10).

3.4. Metabolomics profiling

Untargeted, global metabolomics was employed to characterize any alterations in metabolic activity of liver and kidney cells following glyphosate exposure. The datasets contained a total of 496 biochemicals with known identity in liver cells and 151 biochemicals in kidney cells. Following normalization to dsDNA concentration, log transformation and imputation of missing values, Welch's two-sample t-tests were used to identify biochemicals that differed significantly. Thirty-eight biochemicals in liver cells achieved statistical significance (31 increased and 7 decreased, P ≤ 0.05) and 46 that were approaching significance (42 increased and 4 decreased, 0.05 < P < 0.10). In kidney cells, glyphosate exposure produced significant changes in only 3 metabolites (3 increased and 0 decreased, P ≤ 0.05), while 6 biochemicals showed a trend toward significance (5 increased and 1 decreased, 0.05 < P < 0.10) (Table 2).

Several polyunsaturated fatty acids (PUFAs) were significantly (P ≤ 0.05) elevated in hepatocytes exposed to glyphosate, i.e. linoleate (18:2n6), linolenate 18:3n3, heneicosapentaenoic acid, hexadecadienoate (16:2n6), stearidonate (18:4n3), docosapentaenoate (n3 DPA; 22:5n3), dihomo-linolenate (20:3n3), arachidonate (20:4n6) and docosapentaenoate (n6 DPA; 22:5n6). In addition, eicosapentaenoate (EPA; 20:5n3), docosahexaenoate (DHA; 22:6n3) and docosatrienoate (22:3n6) were trending towards being significantly elevated. (0.05 < P < 0.10) (Fig. 9A and supplementary). The levels of several long-chain fatty acids were likewise higher in glyphosate exposed hepatocytes compared to vehicle controls i.e. pentadecanoate (15:0), palmitoleate

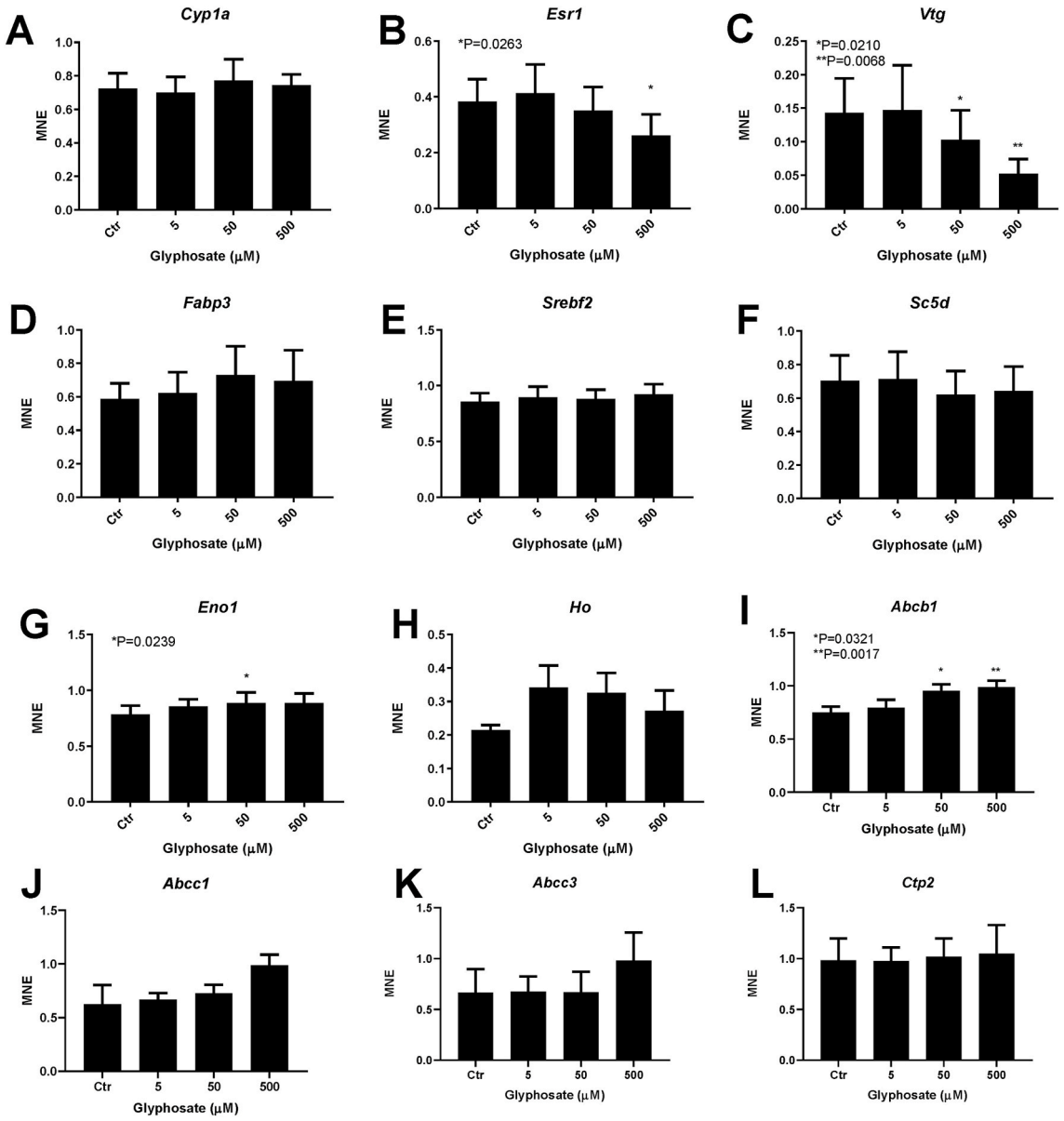

Fig. 5. Transcriptional dose-response relationships for 3D hepatocytes co-cultured with kidney cells exposed to glyphosate. A) *Cyp1a*, B) *Esr1*, C) *Vtg*, D) *Fabp3*, E) *Srebf2*, F) *Sc5d5*, G) *Eno1*, H) *Ho* I) *Abcb1*, J) *Abcc1*, K) *Abcc3* and L) *Cpt2*. Cells were isolated from six male Atlantic salmon (N = 6). Asterisks over bar indicate statistical differences between control and different exposure groups (one-way ANOVA with Dunnett's post-test, mean ± SEM, **P < 0.01 and * P < 0.05).

(16:1n7) and 10-heptadecenoate (17:1n7) ($P \leq 0.05$). The results also showed a trend that the fatty acids oleate/vaccenate (18:1) and myristate (14:0) were increased $0.05 < P < 0.10$) (Fig. 9B and supplementary). Glyphosate exposure further affected histidine metabolism in the hepatocytes, with higher levels of imidazole lactate ($P \leq 0.05$), slightly higher histidine levels ($P = 0.09$), and lower levels of formiminoglutamate and hydantoin-5-propionic acid ($P \leq 0.05$) in exposed cells compared to vehicle controls (Fig. 9C and supplementary).

Liver and kidney biochemicals with $P \leq 0.05$ and $0.05 < P < 0.10$, respectively, were used in the IPA analysis (Table 2). The top molecular and cellular functions in the IPA analysis that is based on metabolites and target genes transcripts (Table 3) predicted effect on the lipid metabolism, molecular transport and small molecule biochemistry in both liver and kidney cells. In the liver, the top four molecules with increased concentrations were *Abcc1* (fold-change (FC) 3.64), folic acid (FC 2.22), (all z)-7,10,13,16,19-docosapentanodic acid (FC 1.69) and arachidonic acid (FC 1.66), while the top 3 molecules with reduced levels were maltotriose (FC -2.00), glycerylphosphoinositol (FC -1.89), and sn-glycerol-3-phosphate (FC -1.82) (Table 4). According to the IPA, 8 individual molecules (Table 4) that were increased in exposed kidney cells, the top three were propionylcarnitine (FC 8.49), urea (FC 6.17) and spermidine (FC 3.11). Cholesterol and L-histidine were also elevated with a FC of 2.66 and 2.02, respectively. *Clu* was the only molecule that was decreased (FC-22.63) in glyphosate exposed kidney cells.

The top toxicological pathways in liver cells were glutathione depletion (based on *Cyp* induction and reactive metabolites), hepatic cholestasis, constitutive androstane receptor.

(Car)/retinoid X receptor *(Rxr)* activation, xenobiotic metabolism signaling and renal necrosis/cell death. The top toxicological pathways in kidney cells were protection from hypoxia-induced renal ischemic injury, renal safety biomarker panel, long-term renal injury anti-oxidative response panel, positive acute phase response proteins, and increases cardiac proliferation. Hepatotoxicity pathways affected were linked to liver damage, liver cholestasis, hepatocellular carcinoma, liver hyperplasia/hyperproliferation and liver cirrhosis. Nephrotoxicity pathways afflicted were kidney failure, renal damage, renal

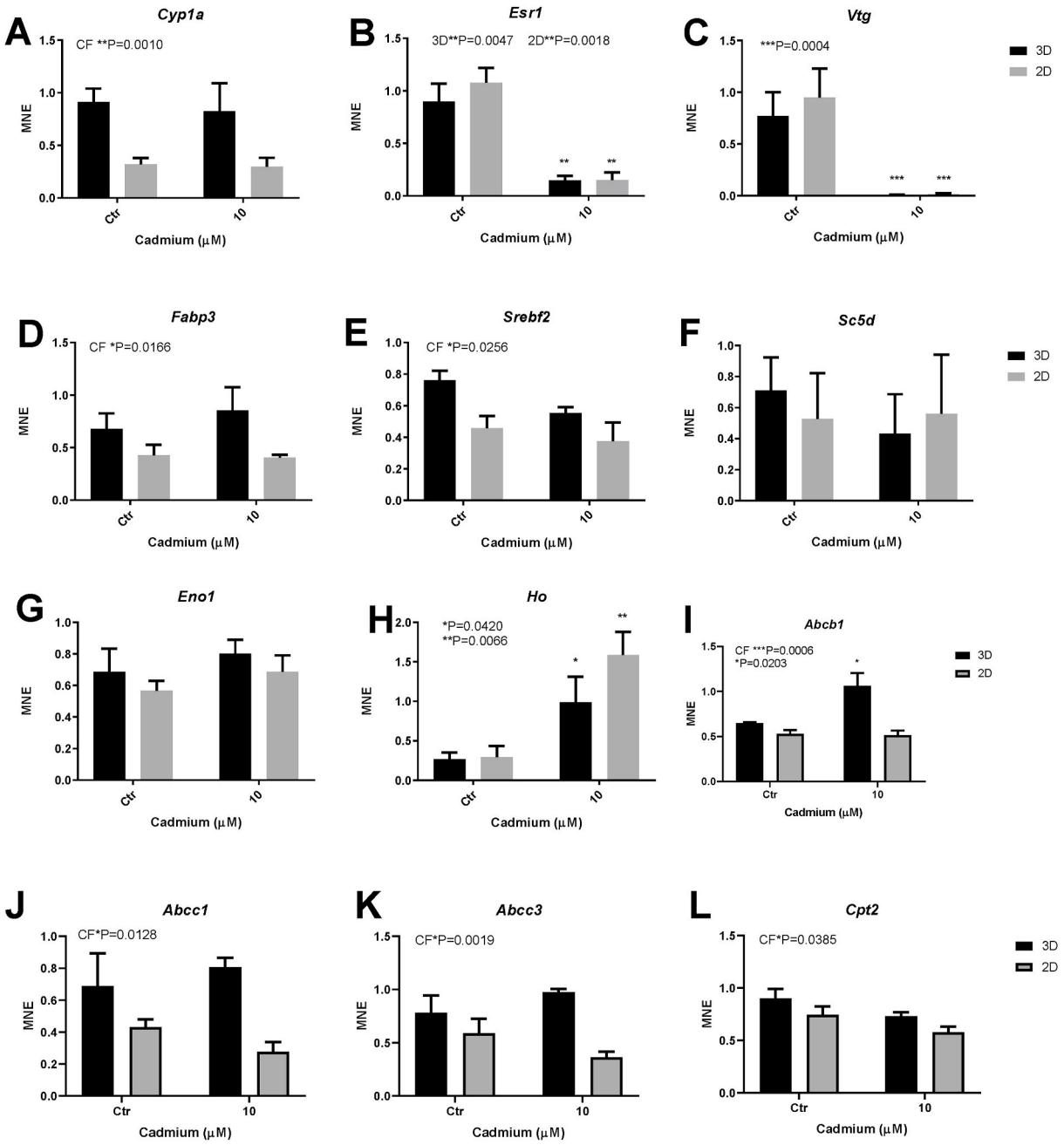

Fig. 6. Transcriptional dose-response relationships for 2D and 3D hepatocytes co-cultured with kidney cells exposed to cadmium. A) *Cyp1a* B) *Esr1*, C) *Vtg*, D) *Fabp3*, E) *Srebf2*, F) *Sc5d5*, G) *Eno1*, H) *Ho* I) *Abcb1*, J) *Abcc1*, K) *Abcc3* and L) *Cpt2*. Cells were isolated from three male Atlantic salmon (N = 3). Asterisks over bar indicate statistical differences between control and different exposure groups (two-way ANOVA with Tukey post-test, mean ± SEM, ***P < 0.001, **P < 0.01 and * P < 0.05). Cell system factor (CF).

inflammation, renal nephritis, and glomerular injury (Table 3).

4. Discussion

3D co-culture models permit the study of cellular responses, mimicking organ-specific *in vivo* cells. However, few advanced Atlantic salmon co-culture models exist today, primarily due to lack of commercially available 3D scaffolds that can be used to cultivate cells at low temperature. 2D primary Atlantic salmon hepatocytes have been successfully applied in investigations of mode of action of contaminants (Olsvik et al., 2015, 2017; Søfteland et al., 2009, 2014) and co-cultured with primary head kidney cells and visceral adipocyte tissue (Holen et al., 2019) and monocytes (Krøvel et al., 2011). In this work a method for isolation and culturing 2D primary Atlantic salmon kidney epithelial cells together with 3D hepatocytes was developed. Specific transcriptional markers for kidney epithelial cells (*Alpl*, *Cd29* and *Cd324*) and light microscopy of freshly isolated, hematoxylin and neutral red stained cells confirmed that the established density gradient method was able to isolate viable proximal tubular and distal tubular cells (Lash, 1996). Havcr1 was significantly upregulated in kidney cells exposed to 10 μM cadmium. HAVCR1 is a protein in the cell membrane with undetermined function that is not expressed in the healthy kidney, but is upregulated in case of renal injury like inflammation and fibrosis (van Timmeren et al., 2007; Vinken et al., 2012). The upregulation of this marker verify that kidney cells isolated with the new method described in this study are responsive to chemical exposure.

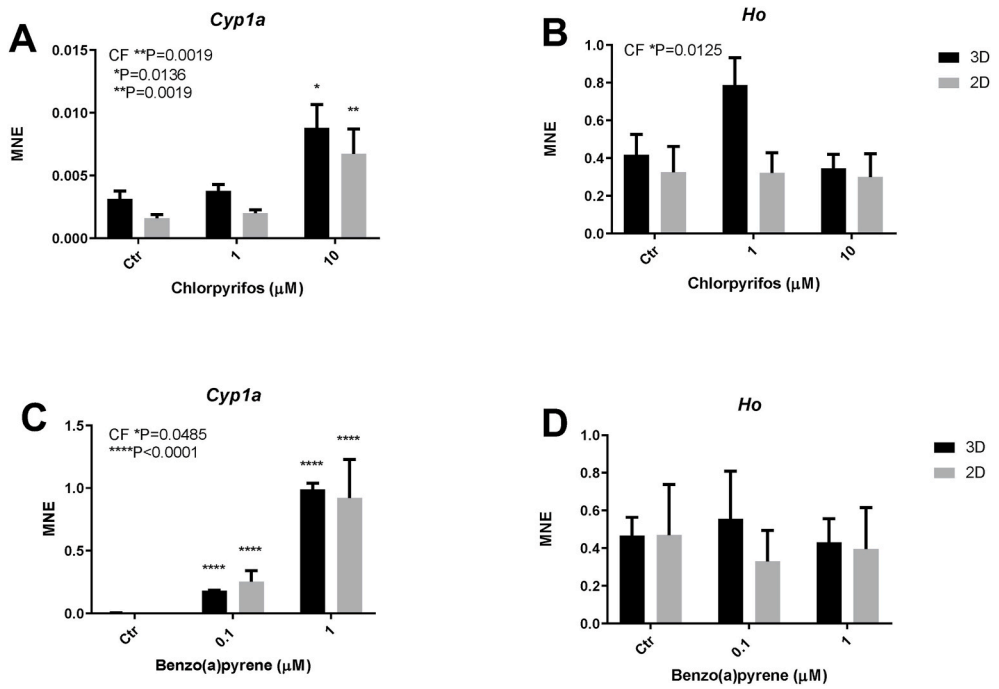

Fig. 7. Transcriptional dose-response relationships for 2D and 3D hepatocytes co-cultured with kidney cells exposed to chlorpyrifos or benzo(a)pyrene. A and C) *Cyp1a*, and B and D) *Ho*. Cells were isolated from three male Atlantic salmon (N = 3). Asterisks over bar indicate statistical differences between control and different exposure groups (two-way ANOVA with Tukey post-test, mean ± SEM, ****P < 0.0001, **P < 0.01 and * P < 0.05). Cell system factor (CF).

To determine if the 2D kidney epithelial cells should be co-cultured with 2D or 3D hepatocytes, hepatocytes were exposed to chlorpyrifos, benzo(a)pyrene and cadmium to evaluate well-known toxic responses produced by the two different cultivation systems. Similar to the findings of Edmondson et al. (2014), no significant cell viability differences were observed between 2D and 3D cultured Atlantic salmon hepatocytes. According to the RT-qPCR analyses, the transcription levels of effected biomarkers *Esr1*, *Vgt* and *Ho* in cadmium exposed cells and *Cyp1a* in chlorpyrifos and benzo(a)pyrene exposed cells were approximately the same, though with the 2D hepatocytes being slightly more sensitive to toxic insult than the 3D cells. The basal transcriptional levels of several other markers were higher in 3D than 2D cultured hepatocytes, which may explain why the 3D cultured hepatocytes were less sensitive than the 2D cultures. The ABCB1 protein is an ATP-dependent pump for removal of xenobiotics from cells and are accountable for reduced accumulation of many xenobiotics (Mahadevan and List, 2004). The transcriptional level of this transporter was significantly increased in 3D cultured hepatocytes exposed to cadmium. Mammalian 3D cell cultures have in many cases been found to be more resilient to drug therapy than 2D cell cultures. In contrast to 2D cell cultures, 3D cells retain the expression of e.g. receptors. Differences in the expression level of receptors and drugs binding efficiency to these receptors between 3D and 2D cell cultures are mainly caused by structural differences and discrepancy in positioning of cell surface receptors. 2D monolayer cultivation are abnormal and stressful for cells causing expression alteration of some genes and proteins in contrast to 3D cell cultures that display gene and protein expression profiles that resembles more closely *in vivo* condition, with improved prediction of drug responses *in vivo* (Edmondson et al., 2014). Thus, the current results obtained with 3D cultured Atlantic salmon hepatocytes support previous studies. Cells cultivated on 3D polystyrene scaffolds displayed improved performance and function compared to 2D cell cultivation during drug and toxicological challenge (Bokhari et al., 2007; Schutte et al., 2011). Consequently, it was decided to use 3D cultured hepatocytes in a co-culture with 2D cultured kidney epithelial cells in downstream toxicity assessments.

For further evaluation of the responsiveness of the 3D hepatocyte-kidney epithelial co-culture, cells were exposed to the glyphosate, a herbicide often found enriched in salmon aquafeed. The transcriptional analysis showed that the multidrug resistance *Abcb1* transporter was significantly upregulated in cells exposed to 50 µM and 500 µM glyphosate, suggesting that the hepatocytes attempt to alleviate the toxicity by transporting glyphosate out of the cells. The global metabolomic analysis showed that non-cytotoxic concentration of glyphosate (500 µM) caused liver and kidney toxicity. In line with these results, water exposure of the Asian stinging catfish (*Heteropneustes fossilis*) to sublethal doses of glyphosate (17.20 mg/l, or approximately 102 µM) for 30 days triggered enlarged, irreversible damage to the liver, necrosis, and accumulation of fat and kidney deteriorating effects on glomeruli, distal and proximal tubule, and the epithelial lining (Samanta et al., 2016). Similar liver and kidney cell damage and necrosis, non-alcoholic fatty liver (accumulation of lipids) and inflammation have also been observed in glyphosate and glyphosate-based herbicides exposed mammals (Gill et al., 2018; Mesnage et al., 2017a, 2022). In plants, glyphosate induces toxicity by functioning as an antagonist of 5-enolpyruvylshikimate-3--phosphate synthase (EPSPS) (Gill et al., 2018) by competing and binding stronger to phosphoenolpyruvate binding site of the EPSPS enzyme than phosphoenolpyruvate (Schönbrunn et al., 2001). Phosphoenolpyruvate is also an important biochemical in animals where it participates in the glycolysis and gluconeogenesis (Metabolome Database, 2021). In the glycolysis pathway, phosphoenolpyruvate is produced by the enzyme ENO1 (Didiasova et al., 2019) and the transcript encoding ENO1 was significantly upregulated in primary Atlantic salmon hepatocytes exposed to 50 µM glyphosate. In earlier *in vivo* glyphosate studies, increased glucose levels (Gill et al., 2018; Li et al., 2016) and decreased amount of glycogen droplets (Samanta et al., 2016) have been reported in the liver of fish. The metabolomic analysis in the present study disclosed dysregulation of lipid metabolism in both liver and kidney cells after glyphosate exposure. The perturbation pattern of lipid metabolism in hepatocytes exposed to 500 µM glyphosate suggests a switch from glycolysis to initiation of gluconeogenesis (Ellingwood and Cheng, 2018; Tadaishi et al., 2018) which can explain why *Enol* was only

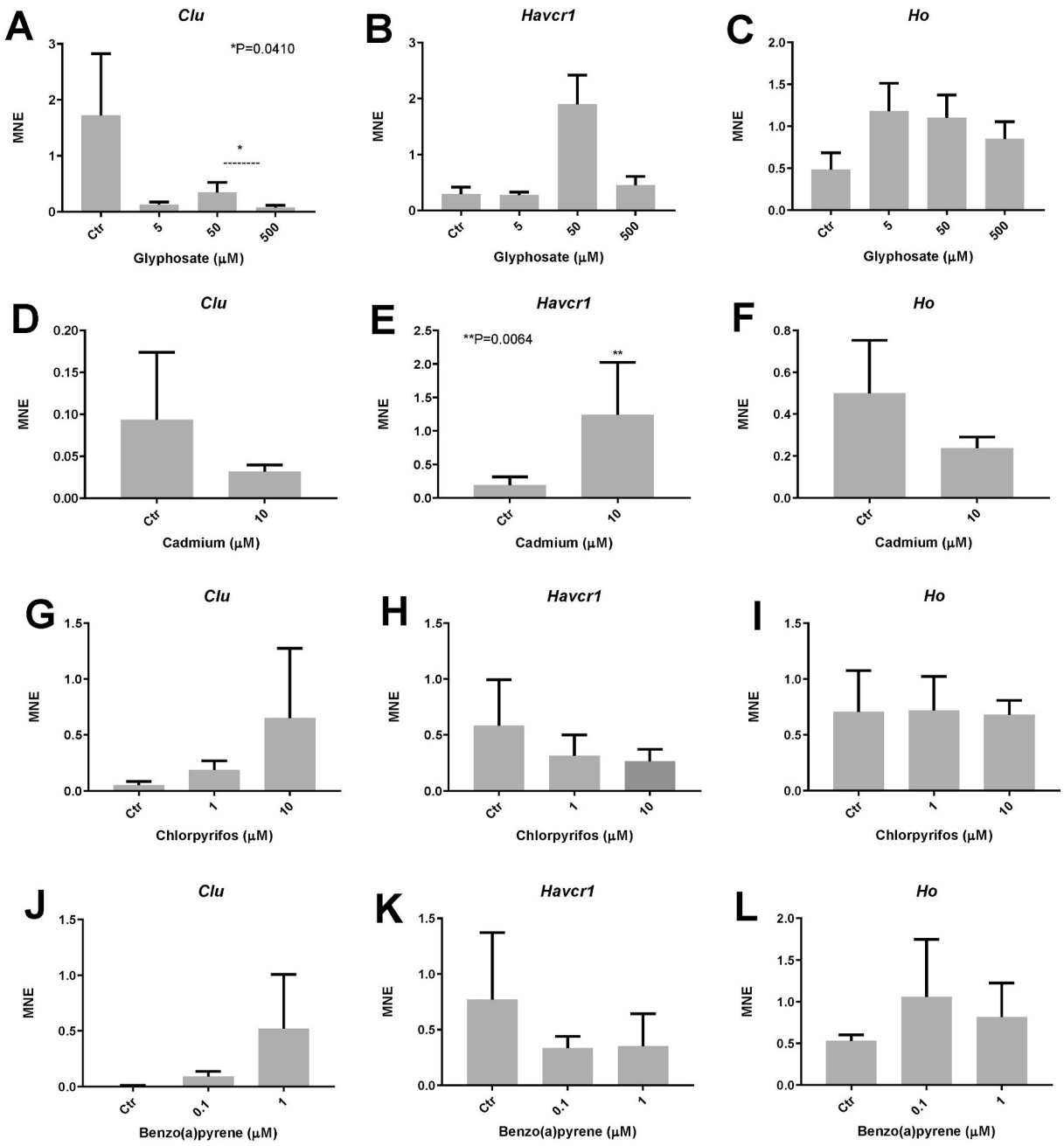

Fig. 8. Transcriptional dose-response relationships for 2D kidney cells co-cultured with and 3D hepatocytes exposed to glyphosate (N = 6), cadmium (N = 3), chlorpyrifos (N = 3) or benzo(a)pyrene (N = 3). A, D, G and J) *Clu*) B, E, H and K) *Havcr1*) and C, F, I and L) *Ho*). Asterisks over bar indicate statistical differences between control and different exposure groups (one-way ANOVA with Tukey's post-test and paired T-test, two-tailed, mean ± SEM, **P < 0.01 and * P < 0.05).

Table 2
Significantly altered biochemicals in liver and kidney cells exposed to glyphosate (500 µM).

Significantly altered biochemicals	Liver cells Glyphosate 500 µM	Kidney cells Glyphosate 500 µM
Total biochemicals P ≤ 0.05	38	3
Biochemicals (↑|↓)	31|7	3|0
Total biochemicals 0.05 < P< 0.10	46	6
Biochemicals (↑|↓)	42|4	5|1

elevated at 50 µM glyphosate. In support of this, glyphosate reduced the levels of glycerol 3-phosphate in the hepatocytes which is a chemical intermediate generated in the glycolysis metabolic pathway that previously has been shown to be reduced during fasting (Martins-Santos et al., 2007). Further, two peroxisome proliferator-activated receptor α (PPARα) inducers, oleoylethanolamide and palmitoylethanolamide, were elevated 1.5 and 1.58-fold, respectively, in the hepatocytes. PPARα encodes a key transcription regulator of liver lipid metabolism. Under energy shortage, PPARα stimulates uptake, consumption, and fatty acid catabolism by transcriptional activation of genes important for binding, activation and transport of fatty acids and mitochondrial and peroxisomal β-oxidation of fatty acids (Kersten et al., 1999). Oleoylethanolamide binding to PPARα promotes lipolysis and the production of glycerol and fatty acids via triglycerides hydrolysation (Duncan et al., 2007; Gaetani et al., 2008). In a 30-day Roundup trial with brown trout (*Salmo trutta*), 10 and 20 mg/l of the glyphosate-containing herbicide reduced the levels of eicosapentaenoic acid (20:5n3) and

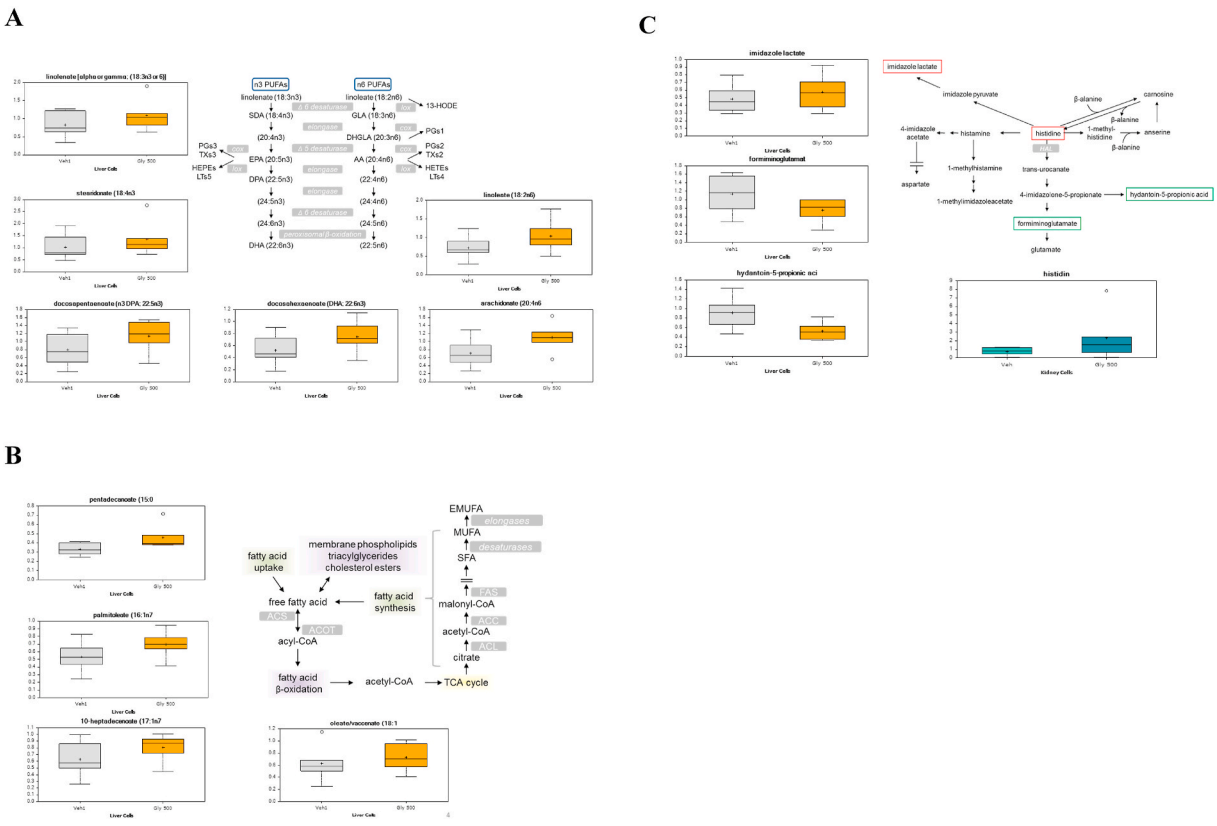

Fig. 9. Biochemical metabolites affected in Atlantic salmon liver cells and kidney cells exposed to glyphosate: A) Polyunsaturated fatty acids (PUFAs), B) Long-chain fatty acids and C) Histidine metabolism. Cells were isolated from six male Atlantic salmon (N = 6). Affected metabolites are presented as box plots with median values and max and min distributions and is based on Welch's two-sample t-tests ($P < 0.05$). Extreme data points are indicated with a circle.

docosahexaenoate (22:6n3) due to fatty acids oxidation (Bayir et al., 2013). Decrease levels of free long-chain fatty acids and PUFAs were measured in HepaRG human liver cells exposed to 0.06 μM of glyphosate, with no effects observed at 6 and 600 μM (Mesnage et al., 2018). Several types of PUFAs and long-chain fatty acids like pentadecanoate (15:0), palmitoleate (16:1n7), 10-heptadecenoate (17:1n7), oleate/vaccinate (18:1) were however elevated in the Atlantic salmon hepatocytes when exposed to the pure glyphosate compound in this study. There are multiple possibilities to explain higher PUFA and long-chain fatty acids levels in hepatocytes exposed to glyphosate, including increased de novo synthesis, increased uptake from media, increased lipase activity on phospholipids, and decreased fatty acid beta-oxidation. The PUFAs linolenate (18:3n3) and linoleate (18:2n6), essential fatty acids that are acquired through the diet, were elevated in the glyphosate-treated cells, probably reflecting increased uptake from the media since they cannot be synthesized in animal cells (Tocher, 2003). Other PUFAs, such as stearidonate (18:4n3), docosapentaenoate (22:5n3), and arachidonate (20:4n6) can be synthesized through the concerted activity of elongases and desaturases and most of the measured PUFAs in this study were elevated. Docosahexaenoate, which is synthesized through beta-oxidation of 24-carbon containing PUFA (Tocher, 2003), showed a trend toward significance. The elevation of PUFAs in liver cells in the present study could be consistent with increased elongase and desaturase activity resulting from glyphosate treatment. However, lipid synthesis is normally inhibited during starvation (Torstensen et al., 2001). Since there were no significant effects on fatty acid beta oxidation markers e.g. 3-hydroxybutyrate ((Mierziak et al., 2021), the *Cpt2* transcript (Barerro et al., 2003; Torstensen et al., 2001) or TCA cycle intermediates (Houten and Wanders, 2010), the increased levels of lipids must therefore be caused by higher rates of phospholipid hydrolysis. Organophosphate (e.g. chlorpyrifos-methyl and pirimiphos-methyl) and organochlorine pesticides have previously been shown to cause disturbed phospholipid and/or triacylglycerol synthesis (Berntssen et al., 2021, Sanden et al., 2018; Krøvel et al., 2010; Glover et al., 2007). In contrast to chlorpyrifos-methyl and pirimiphos-methyl, which have log Kow of 4.12 and 4.31, respectively (Berntssen et al., 2021), the log Kow for glyphosate is -3.4 (PubChem database, 2021) and glyphosate is thus a very hydrophilic compound (Cumming and Rücker, 2017). Exposure to lipid-soluble pesticides *in vivo* have resulted in reduced levels of n-6 PUFAs like arachidonic acid (20:4n-6) and increased levels of saturated fatty acids like palmitic acid (16:0) in Atlantic salmon (Berntssen et al., 2021; Sanden et al., 2018). Both studies explained these effects to be caused by homoviscous adaption (Levental et al., 2020; Levental and Levental, 2019; Sinensky, 1974), and/or lipid peroxidation (Cengiz et al., 2016; Berntssen et al., 2021). Since glyphosate is not lipophilic, a more plausible explanation for the observed lipid stress could be phospholipid remodelling (Lands, 1958; Sanden et al., 2018) caused by enhanced phospholipase A (PLA_2) and reduced lysophospholipid acyltransferase (LPLAT) activity. This would affect the quantity of membrane phospholipids and increase the level of lysolipids and free fatty acids. Increases in PUFAs such as arachidonate (a metabolite of arachidonic acid (PubChem database, 2021)) can impact the production of prostaglandins, leukotrienes and eicosanoids through the activity of lipoxygenase and cyclooxygenase enzymes (Tocher, 2003; Astudillo et al., 2019), that consequently cause inflammation and membrane destruction (Sanden et al., 2018; Astudillo et al., 2019). Hydrolysis of phospholipids (Pla_2) can also increase the levels of free eicosapentaenoic acid (20:5n3), docosahexaenoate, docosapentaenoate and 16:1n7 (palmitoleic acid), which where all found increased in glyphosate exposed hepatocytes, and can prevent the negative effects of arachidonic acid eicosanoids (Bolsoni-Lopes et al., 2013; Astudillo et al., 2019). In support of the phospholipid remodelling theory, $cPla_2$ and the levels of arachidonic acid produced eicosanoids were found significantly increased in kidney of glyphosate exposed mice

Table 3
Pathways affected in Atlantic salmon liver and kidney cells exposed to glyphosate (500 μM). Pathway analysis is based on significantly affected transcripts and metabolites.

Pathway analysis	*Liver cells GLY* 500 μM	Score/ p-value	*Kidney cells GLY* 500 μM	Score/ p-value
Top canonical pathway	Histidine Degradation VI	2.60E-07	Histamine Biosynthesis	9.24E-04
	tRNA Charging	1.05E-06	Hypusine Biosynthesis	1.54E-03
	4-hydroxybenzoate Biosynthesis	5.60E-06	Spermine Biosynthesis	2.15E-03
	Thiamin Salvage III	4.77E-05	Spermidine Biosynthesis I	2.15E-03
	Phenylalanine Degradation IV	5.82E-05	Heme Degradation	3.38E-03
Top Upstream Regulators	Afatinib (inhibited)	2.07E-18	Sodium chloride	1.50E-06
	Sirolimus (inhibited)	1.05E-10	Soy isoflavones	4.05E-06
	EGFR	1.51E-10	HP	4.05E-06
	SLC22A6	3.36E-08	Cypermethrin	4.05E-06
	N-propyl bromide	4.25E-08	KDM3A	6.18E-06
Top Molecular and Cellular Functions	Lipid Metabolism	4.41E-03 - 7.71E-12	Lipid Metabolism	2.35E-02 – 4.47E-06
	Molecular Transport	4.41E-03 - 7.71E-12	Molecular Transport	2.38E-02 – 4.47E-06
	Small Molecule Biochemistry	4.41E-03 - 7.71E-12	Small Molecule Biochemistry	2.35E-02 – 4.47E-06
	Free Radical Scavenging	2.88E-03 – 8.27E-12	Cell Signaling	2.26E-02 - 5.57E-06
	Cellular Growth and Proliferation	4.41E-03 - 1.62E-10	Post-Translational Modification	1.13E-02 – 1.10E-05
Top tox	Glutathione Depletion - CYP Induction and Reactive Metabolites	3.12E-04	Protection from Hypoxia-induced Renal Ischemic Injury (Rat)	1.23E-03
	Hepatic Cholestasis	7.79E-04	Renal Safety Biomarker Panel (PSTC)	1.85E-03
	CAR/RXR Activation	1.87E-03	Long-term Renal Injury Anti-oxidative Response Panel (Rat)	5.53E-03
	Xenobiotic Metabolism Signaling	7.38E-03	Positive Acute Phase Response Proteins	9.20E-03
	Renal Necrosis/Cell Death	8.81E-03	Increases Cardiac Proliferation	1.50E-02
Hepatotoxicity/ Nephrotoxicity	Liver Damage	9.28E-02 - 6.04E-05	Kidney Failure	5.41E-02 - 1.62E-06
	Liver Cholestasis	3.05E-02 - 3.68E-04	Renal Damage	7.06E-03 – 1.70E-05
	Hepatocellular carcinoma	9.88E-02 - 7.71E-04	Renal Inflammation	1.16E-02 - 6.16E-04
	Liver Hyperplasia/ hyperproliferation	1.00E-00 - 7.71E-04	Renal Nephritis	1.16E-02 - 6.16E-04
	Liver Cirrhosis	1.54E-02 - 1.33E-03	Glomerular Injury	1.16E-02 – 1.28E-03

The Ingenuity pathway analyse used PubChem (a database on biological active molecules) and Human Metabolome Database (HMDB) and Human Gene Symbols (Hugo/HGNC ID, Entrez Gene ID/KEGG) mapped entities. IPA input: Liver: 82 out of 97 biochemicals/genes, kidney: 9 out of 12 biochemicals/genes.

and was suggested to be the mode of action for the observed renal tubular injuries (Wang et al., 2021). The metabolomics data proved that also another membrane associated phospholipase, N-acyl-phosphatidylethanolamine-hydrolysing phospholipase D, was affected by the glyphosate treatment and this phospholipase is responsible and/or involved in the production of the PPARα inducers oleoylethanolamide and palmitoylethanolamide (Zhu et al., 2011; Ueda et al., 2013). Oleoylethanolamide and palmitoylethanolamide are produced as a response to inflammation and injury of cells, possibly as a protecting measure (Hansen et al., 2015). Elevation of palmitoleic acid in the glyphosate-exposed hepatocytes can lead to increased adipocyte lipolysis and lipases by a mechanism that requires a functional PPARα (Bolsoni-Lopes et al., 2013). PPARα has together with PPARγ, another important lipid regulator (Varga et al., 2011), been suggested to be involved in the lipid disturbances (lipid accumulation and increased levels of free fatty acids) measured in common carp (*Cyprinus carpio)* exposed for 45 days to 5 mg/l glyphosate (Liu et al., 2021). Similar to prior studies the present results suggest that high concentrations of glyphosate can disturb cells membrane fluidity in Atlantic salmon liver cells by affecting the activity of phospholipases and lysophospholipid acyltransferases, and cause lipid toxicity through a PPAR(α) mediated pathway.

Cholesterol is structurally important for the integrity of cell membranes. Changes in cholesterol levels can influence the structure of cell membranes and the synthesis of steroids and bile acids. Earlier studies have demonstrated that hydrophobic contaminants can disturb cholesterol homeostasis in Atlantic salmon (*in vitro* and *in vivo*) and in mammals (Edling et al., 2009; Olsvik et al., 2017; Sanden et al., 2018). The metabolomic and RT-qPCR analysis (*Srebf2* and *Sc5d*, cholesterol biosynthesis) of glyphosate-treated hepatocytes did not reveal any perturbation of the cholesterol homeostasis. However, glyphosate exposure increased cholesterol levels in kidney cells. Further, CLU, a protein that participates in preventing stress-induced apoptosis by improving the integrity of the mitochondrial membrane (Li et al., 2013), was significantly downregulated in 500 μM glyphosate exposed kidney cells. The increased levels of cholesterol and downregulation of *Clu* suggest that the kidney cells are trying to prevent renal injury by increasing cholesterol to stabilising cell membranes at these non-cytotoxic concentrations.

Disruption of steroidogenic biosynthesis pathway and reproductive toxicity have been linked to glyphosate exposure in zebrafish (Webster et al., 2014). VTG, an egg-yolk protein precursor produced in female fish liver under estrogenic stimulation of ovarian follicle development (Hinton et al., 2008), can be produced in liver of male fish after exposure to exogenous estrogens. VTG is thus an acknowledged biomarker of endocrine disruption (Navas and Segner, 2006). ESR1 has a key role in the transcriptional upregulation of *Vtg* (Meucci and Arukwe, 2006). In glyphosate-exposed male Atlantic salmon hepatocytes, *Esr1* was

Table 4
Top molecules affected in primary Atlantic salmon liver and kidney cells exposed to glyphosate (500 μM).

Top molecules	*Molecules upregulated*	Fold Change	*Molecules downregulated*	Fold Change
Liver cells	*Abcc1*	3.636	Maltotriose	−2.000
	Folic acid	2.220	Glycerylphosphoinositol	−1.887
	(AllZ)-7,10,13,16,19-docosapentaenoic acid	1.690	Sn-glycerol-3-phosphate	−1.818
	Arachidonic acid	1.660	N-acetyl-L-aspartic acid	−1.724
	Abcc3	1.587	Hydantoin-5-propionate	−1.695
	Palmitoylethanolamide	1.580	ESR1	−1.564
	Thiamine	1.570	Pantetheine	−1.538
	Docosahexaenoic acid	1.530	5-imidazolepropionic acid	−1.493
	Oleoylethanolamide	1.510	Formiminoglutamic acid	−1.471
Kidney cells	Propionylcarnitine	8.490	*Clu*	−22.634
	Urea	6.170		
	Spermidine	3.110		
	3-amino-2,6-piperidinedione	2.800		
	Cholesterol	2.660		
	L-histidine	2.020		
	Ho	1.769		
	Havcr1	1.556		

The Ingenuity pathway analyse used PubChem (a database on biological active molecules) and Human Metabolome Database (HMDB) and Human Gene Symbols (Hugo/HGNC ID, Entrez Gene ID/KEGG) mapped entities. IPA input: Liver: 82 out of 97 biochemicals/genes, kidney: 9 out of 12 biochemicals/genes.

downregulated at the highest concentration (500 μM) and a dose-dependent down-regulation were seen for *Vtg* transcription after 48 h. In line with this finding, estrogen receptor inhibition was observed in human HepG2 cells exposed to a non-cytotoxic concentration of glyphosate (2 ppm or 11.83 μM) (Gasniera et al., 2009). Contrarily, high concentrations of glyphosate have been shown to induce *Esr1* in the breast cancer cell model MCF-7. Since glyphosate possessed only an unstable and weak binding to the ESR1 receptor, Mesnage et al. (2017b) proposed that the activation had to be via a ligand-independent pathway. A similar suppression of *Esr1*, as seen in the present study, has been observed in mice exposed to the PPARα inducer phthalate ester DEHP and the down-regulation of *Esr1* was lost in PPARα-knockout mice (Xi et al., 2020). This suggests that glyphosate-induced suppression of *Esr1* in Atlantic salmon hepatocytes could be due to upregulation of *Pparα*.

Salmonid tissue contains excessive levels of histidine (and histidine derivatives), an essential amino acid with important metabolic and cellular function that are acquired through the feed. (Moro et al., 2020, Remø et al., 2014). In glyphosate exposed Atlantic salmon hepatocytes, changes were noted in histidine metabolism. Higher levels of imidazole lactate, slightly higher histidine levels ($P = 0.09$), and lower levels of formimino-glutamate and hydantoin-5-propionic acid were found in glyphosate exposed hepatocytes. Also, histidine levels showed a trend towards increase in kidney cells exposed to glyphosate ($P = 0.09$). Overall, histidine catabolism downstream of histidase, which catalyzes the reaction of histidine to trans-urocanate (pathway responsible for the production of formimino-glutamate and hydantoin-5-propionic acid), were reduced. The increased levels of imidazole lactate suggest elevation of transamination, which usually are a minor histidine catabolism pathway. An increase in this pathway have previously been seen with prevalence of histidase inhibition (Bender, 2012; Moro et al., 2020). Histidase, found mainly in liver and skin, generate urocanic acid that is further converted by urocanate hydratase to 4, 5-dihydri-4-oxo-5-imidazolepropanoic acid which is again transformed to formimino-glutamate and N5-formimino-tetrahydro-folate. Investigations have shown that estrogen can regulate the activity of histidase (Moro et al., 2020). The observed inhibition of histidase can therefore be a response to the downregulation of *Esr1*. This should be further investigated, to see if one or several enzymes in the histidine pathway are affected by glyphosate exposure.

To our knowledge toxicokinetic data for glyphosate in Atlantic salmon and other fish are lacking, thus the current 3D *in vitro* study focuses on mode of action of glyphosate toxicity in Atlantic salmon. To be able to evaluate if the recently documented glyphosate concentrations in fish feed pose a hazard for the Atlantic salmon, additional *in vivo* dose-response studies are needed to assess effect concentration levels.

In conclusion, the established density gradient method was able to isolate viable and responsive primary salmon kidney cells. The toxicological comparison of 2D with 3D cultured primary hepatocytes demonstrated that the 3D cultured hepatocytes responded superior to the 2D hepatocytes. Glyphosate treatment of the 3D hepatocyte-kidney epithelial co-culture disclosed distressed lipid metabolism in both liver and kidney cells. Glyphosate exposure affected saturated and unsaturated fatty acid levels in hepatocytes due to increased uptake and phospholipid remodelling. Further, the hepatocyte results suggest that glyphosate interfered with the histidine metabolism and that glyphosate can cause endocrine disruption. The increased level of cholesterol suggest that glyphosate impact the stability of membranes in Atlantic salmon kidney cells.

CRediT authorship contribution statement

L. Søfteland: Conceptualization, Data curation, Formal analysis, Investigation, Methodology, Resources, Writing – original draft, Writing – review & editing, Project administration. **P.A. Olsvik:** Conceptualization, Resources, Writing – original draft, Writing – review & editing.

Declaration of competing interest

The authors declare that they have no known competing financial interests or personal relationships that could have appeared to influence the work reported in this paper.

Acknowledgements

The authors would like to thank Betty Irgens and Eva Mykkeltvedt for their contribution with the experimental work. This work was funded by the Research Council of Norway , Grant number 244507, Norway.

Appendix A. Supplementary data

Supplementary data to this article can be found online at https://doi.org/10.1016/j.fct.2022.113012.

References

Astudillo, A.M., Balboa, M.A., Balsinde, J., 2019. Selectivity of phospholipid hydrolysis by phospholipase A2 enzymes in activated cells leading to polyunsaturated fatty acid mobilization. Biochim. Biophys. Acta Mol. Cell Biol. Lipids 1864 (6), 772–783. https://doi.org/10.1016/j.bbalip.2018.07.002.

Barerro, M.J., Camarero, N., Marrero, P.F., Haro, D., 2003. Control of human carnitine palmitoyltransferase II gene transcription by peroxisome proliferator-activated receptor through a partially conserved peroxisome proliferator-responsive element. Biochem. J. 369, 721–729. https://doi: 10.1042/BJ20020851.
Bayir, M., Sirkecioglu, A.N., Abdulkadir Bayir, A., Mevlut Aras, M., 2013. Alterations in fatty acids of polar lipids in Salmo trutta on long-term exposure to a glyphosate-based herbicide (Roundup). Pakistan J. Biol. Sci. 16 (20), 1194–1198. https://doi.org/10.3923/pjbs.2013.1194.1198.
Benbrook, C.M., 2016. Trends in glyphosate herbicide use in the United States and globally. Environ. Sci. Eur. 28 (3), 1–15. https://doi.org/10.1186/s12302-016-0070.
Bender, D., 2012. Amino Acid Metabolism, third ed., vol. 305. Wiley-Blackwell, London, England, ISBN 978-1-118-35818-4, p. 322.
Benjamini, Y., Hochberg, Y., 1995. Controlling the False Discovery Rate: of practical and powerful approach two multiple testing. J. R. Stat. Soc. Ser. B Stat. Methodol. 57 (1), 289–300. https://doi.org/10.1111/j.2517-6161.1995.tb02031.x.
Berntssen, M.H.G., Rosenlund, G., Garlito, B., Amlund, H., Sissener, N.H., Bernhard, A., Sanden, M., 2021. Sensitivity of Atlantic salmon to the pesticide pirimiphos-methyl, present in plant-based feeds. Aquaculture 531, 735825. https://doi.org/10.1016/j.aquaculture.2020.735825.
Bhogal, N., Grindon, C., Combes, R., Balls, M., 2005. Toxicity testing: creating a revolution based on new technologies. Trends Biotechnol. 23 (6), 299–307. https://doi.org/10.1016/j.tibtech.2005.04.006.
Bokhari, M., Carnachan, R.J., Cameron, N.R., Przyborski, S.A., 2007. Culture of HepG2 liver cells on threedimensional polystyrene scaffolds enhances cell structure and function during toxicological challenge. J. Anat. 211 (4), 567–576. https://doi.org/10.1111/j.1469-7580.2007.00778.x.
Bols, N.C., Lee, L.E.J., 1991. Technology and uses of cell cultures from the tissues and organs of bony fish. Cytotechnology 6, 163–187.
Bolsoni-Lopes, A., Festuccia, W.T., Farias, T.S.M., Chimin, P., Torres-Leal, F.L., Derogis, P.B.M., de Andrade, P.B., Miyamoto, S., Lima, F.B., Curi, R., Alonso-Vale, M. I.C., 2013. Palmitoleic acid (n-7) increases white adipocyte lipolysis and lipase content in a PPARα-dependent manner. Am. J. Physiol. Endocrinol. Metab. 305 (9), E1093–E1102. https://doi.org/10.1152/ajpendo.00082.2013.
Breslin, S., O'Driscoll, L., 2013. Three-dimensional cell culture: the missing link in drug discovery. Drug Discov. Today 18 (5–6), 240–249. https://doi.org/10.1016/j.drudis.2012.10.003.
Cengiz, E.I., Bayar, A.S., Kizmaz, V., 2016. The protective effect of vitamin E against changes in fatty acid composition of phospholipid subclasses in gill tissue of Oreochromis niloticus exposed to deltamethrin. Chemosphere 147, 138–143.
Cumming, H., Rücker, C., 2017. Octanol-water partition coefficient measurement by a simple 1H NMR method. ACS Omega 2 (9), 6244–6249.
Didiasova, M., Schaefer, L., Wygrecka, M., et al., 2019. When place matters: shuttling of enolase-1 across cellular compartments. Front. Cell Dev. Biol. 26 https://doi.org/10.3389/fcell.2019.00061.
Donato, T., Castell, J.V., Gomez-Lechon, M.J., 1994. Cytochrome p450 activities in pure and co-cultured hepatocytes. Effects of model inducers. In Vitro Cell. Dev. Biol. 30A, 825–832.
Duncan, R.E., Ahmadian, M., Jaworski, K., Sarkadi-Nagy, E., Sul, H.S., 2007. Regulation of lipolysis in adipocytes. Annu. Rev. Nutr. 27 (1), 79101. https://doi.org/10.1146/annurev.nutr.27.061406.093734.
Edling, Y., Sivertsson, L.K., Butura, A., Ingelman-Sundberg, M., Ek, M., 2009. Increased sensitivity for troglitazone-induced cytotoxicity using a human in vitro co-culture model. Toxicol. Vitro 23, 1387–1395.
Edmondson, R., Broglie, J.J., Adcock, A.F., Yang, L., 2014. Three-dimensional cell culture systems and their applications in drug discovery and cell-based biosensors. Assay Drug Dev. Technol. 12 (4), 207–218. https://doi.org/10.1089/adt.2014.573.
Ellingwood, S.S., Cheng, A., 2018. Biochemical and clinical aspects of glycogen storage diseases. J. Endocrinol. 238 (3), R131–R141.
Fent, K., 2001. Fish cell lines as versatile tools in ecotoxicology: assessment of cytotoxicity, cytochrome P4501A induction potential and estrogenic activity of chemicals and environmental samples. Toxicol. Vitro 15, 477–488.
Fischer, A.H., Jacobson, K.A., Rose, J., Zeller, R., 2008. Hematoxylin and eosin staining of tissue and cell sections. Cold Spring Harb. Protoc. https://doi.org/10.1101/pdb.prot4986.
Gaetani, S., Kaye, W.H., Cuomo, V., Piomelli, D., 2008. Role of endocannabinoids and their analogues in obesity and eating disorders. Eat. Weight Disord. 13 (3), e42–e48.
Gasniera, C., Dumontb, C., Benachoura, N., Claira, E., Chagnonb, M.-C., Séralinia, G.-E., 2009. Glyphosate-based herbicides are toxic and endocrine disruptors in human cell lines. Toxicology 262 (3), 184–191. https://doi.org/10.1016/j.tox.2009.06.006.
Gill, J.P.K., Sethi, N., Mohan, A., Datta, S., Girdha, M., 2018. Glyphosate toxicity for animals. Environ. Chem. Lett. 16, 401–426. https://doi.org/10.1007/s10311-017-0689-0.
Glover, C.N., Petri, D., Tollefsen, K.E., Jorum, N., Handy, R.D., Berntssen, M.H.G., 2007. Assessing the sensitivity of Atlantic salmon (Salmo salar) to dietary endosulfan exposure using tissue biochemistry and histology. Aquat. Toxicol. 84, 346–355. https://doi.org/10.1016/j.aquatox.2007.06.013.
Hansen, H.S., Kleberg, K., Hassing, H.A., 2015. Non-endocannabinoid N-acylethanolamines and monoacylglycerols: old molecules new targets. In: Di Marzo, V., Wang, J. (Eds.), The Endocannabinoidome -The World of Endocannabinoids and Related Mediators. Academic Press, Elsevier, Amsterdam, The Netherlands, pp. 1–13.
Hinton, D.E., Segner, H., Au, D.W.T., Kullman, S.W., Hardman, R.C., 2008. Liver toxicity. In: Di Giulio, Hinton, D.E. (Eds.), The Toxicology of Fishes. Taylor and Francis Group, Boca Raton, Florida, pp. 327–400.
Holen, E., Espe, M., Andersen, S.M., Taylor, R., Aksnes, A., Mengesha, Z., Araujo, P., 2014. A co culture approach show that polyamine turnover is affected during inflammation in Atlantic salmon immune and liver cells and that arginine and LPS exerts opposite effects on p38MAPK signaling. Fish Shellfish Immunol. 37 (2), 286–298.
Holen, E., Araujo, P., Xie, S., Søfteland, L., Espe, M., 2019. Resveratrol inhibited LPS induced transcription of immune genes and secretion of eicosanoids in Atlantic salmon (Salmo salar), comparing mono-, co- and a novel triple cell culture model of head kidney leukocytes, liver cells and visceral adipocyte tissue. Comp. Biochem. Physiol. C Toxicol. Pharmacol. 224, 108560. https://doi.org/10.1016/j.cbpc.2019.108560.
Houten, S.M., Wanders, R.J.A., 2010. A general introduction to the biochemistry of mitochondrial fatty acid β-oxidation. J. Inherit. Metab. Dis. 33 (5), 469–477. https://doi.org/10.1007/s10545-010-9061-2.
Huh, D., Hamilton, G.A., Ingber, D.E., 2011. From 3D cell culture to organs-on-chips. Trends Cell Biol. 21 (12), 745–754.
ISO, 2009. Biological evaluation of medical devices Part 5: Tests for in vitro cytotoxicity. International standard. ISO (10993–5), 1–34. https://www.iso.org/standard/36406.html.
Kersten, S., Seydoux, J., Peters, J.M., Gonzalez, F.J., Desvergne, B., Wahli, W., 1999. Peroxisome proliferator-activated receptor alpha mediates the adaptive response to fasting. J. Clin. Invest. 103 (11), 1489–1498. https://doi.org/10.1172/JCI6223.
Krøvel, A.V., Søfteland, L., Torstensen, B.E., Olsvik, P.A., 2010. Endosulfan in vitro toxicity in Atlantic salmon hepatocytes obtained from fish fed either fish oil or vegetable oil. Comp. Biochem. Physiol. C Toxicol. Pharmacol. 151 (2), 175–186. https://doi.org/10.1016/j.cbpc.2009.10.003.
Krøvel, A.V., Winterthun, S., Holen, E., Olsvik, P.A., 2011. Development of a co-culture model for in vitro toxicological studies in Atlantic salmon. Toxicol. Vitro 25 (5), 1143–1152. https://doi.org/10.1016/j.tiv.2011.03.020.
Lands, W.E.M., 1958. Metabolism of glycerolipides - comparison of lecithin and triglyceride synthesis. J. Biol. Chem. 231, 883–888. https://doi.org/10.1016/S0021-9258(18)70453-5.
Langiano, V.D.C., Martinez, C.B.R., 2008. Toxicity and effects of a glyphosate-based herbicide on the Neotropical fish Prochilodus lineatus. Comp. Biochem. Physiol., C 147, 222–231. https://doi.org/10.1016/j.cbpc.2007.09.009.
Lash, L.H., 1996. Use of freshly isolated and primary cultures of proximal tubular and distal tubular cells from rat kidney. In: Zalups, R.K., Lash, L.H. (Eds.), Methods in Renal Toxicology. CRC press, New York, USA, pp. 189–215.
Levental, K.R., Levental, I., 2019. Homeoviscous adaptation in mammalian cell membranes in response to dietary lipid perturbations. Biophys. J. 116, 20A.
Levental, K.R., Malmberg, E., Symons, J.L., 2020. Lipidomic and biophysical homeostasis of mammalian membranes counteracts dietary lipid perturbations to maintain cellular fitness. Nat. Commun. 11, 1339. https://doi.org/10.1038/s41467-020-15203-1.
Li, T., Chiang, J.Y.L., 2009. Regulation of bile acid and cholesterol metabolism by PPARs. PPAR Res. 501739 https://doi.org/10.1155/2009/501739.
Li, M.-H., Xu, H.-D., Liu, Y., Chen, T., Jiang, L., Fu, Y.-H., Wang, J.-S., 2016. Multi-tissue metabolic responses of goldfish (Carassius auratus) exposed to glyphosate-based herbicide. Toxicol. Res. 5, 1039. https://doi.org/10.1039/c6tx00011h.
Li, N., Zoubeidi, A., Beraldi, E., Gleave, M.E., 2013. GRP78 regulates clusterin stability, retrotranslocation and mitochondrial localization under ER stress in prostate cancer. Oncogene 32, 1933–1942. https://doi.org/10.1038/onc.2012.212.
Liu, J., Dong, C., Zhai, Z., Tang, L., LinWang, L., 2021. Glyphosate-induced lipid metabolism disorder contributes to hepatotoxicity in juvenile common carp. Environ. Pollut. 269, 116186. https://doi.org/10.1016/j.envpol.2020.116186.
Mahadevan, D., List, A.F., 2004. Targeting the multidrug resistance-1 transporter in AML: molecular regulation and therapeutic strategies. Blood 104 (7), 1940–1951. https://doi.org/10.1182/blood-2003-07-2490.
Martins-Santos, M.E.S., Chaves, V.E., Frasson, D., Boschini, R.P., Garofalo, M.A.R., Kettelhut, I.C., Migliorini, R.H., 2007. Glyceroneogenesis and the supply of glycerol-3-phosphate for glyceride-glycerol synthesis in liver slices of fasted and diabetic rats. Am. J. Physiol. Endocrinol. Metab. 293, E1352–E1357. https://doi.org/10.1152/ajpendo.00394.2007.
Mesnage, R., Renney, G., Séralini, G.-E., Ward, M., Antoniou, M.N., 2017a. Multiomics reveal non-alcoholic fatty liver disease in rats following chronic exposure to an ultra-low dose of Roundup herbicide. Sci. Rep. 7, 39328. https://doi.org/10.1038/srep39328.
Mesnage, R., Phedonos, A., Biserni, M., Arno, M., Balu, S., Corton, J.C., Ugarte, R., Antoniou, M.N., 2017b. Evaluation of estrogen receptor alpha activation by glyphosate-based herbicide constituents. Food Chem. Toxicol. 108 A, 30–42. https://doi.org/10.1016/j.fct.2017.07.025.
Mesnage, R., Biserni, M., Wozniak, E., Xenakis, T., Mein, C.A., Antoniou, M.N., 2018. Comparison of transcriptome responses to glyphosate, isoxaflutole, quizalofop-p-ethyl and mesotrione in the HepaRG cell line. Toxicol Rep 5, 819–826. https://doi.org/10.1016/j.toxrep.2018.08.005.
Mesnage, R., Ibragim, M., Mandrioli, D., Falcioni, L., Tibaldi, E., Belpoggi, F., Brandsma, I., Bourne, E., Savage, E., Mein, C.A., Michael, N., Antoniou, M.N., 2022. Comparative toxicogenomics of glyphosate and Roundup herbicides by mammalian stem cell-based genotoxicity assays and molecular profiling in Sprague Dawley rats. Toxicol. Sci. 186 (1), 83–101. https://doi.org/10.1093/toxsci/kfab143.
Metabolome Database, 2021. https://hmdb.ca/metabolites/HMDB0000263.
Meucci, V., Arukwe, A., 2006. Transcriptional modulation of brain and hepatic estrogen receptor and P450arom isotypes in juvenile Atlantic salmon (Salmo salar) after waterborne exposure to the xenoestrogen, 4-nonylphenol. Aquat. Toxicol. 77 (2), 167–177, 2006.
Mierziak, J., Burgberger, M., Wojtasik, W., 2021. 3-Hydroxybutyrate as a metabolite and a signal molecule regulating processes of living organisms. Biomolecules 11, 402. https://doi.org/10.3390/biom11030402.

Moro, J., Tomé, D., Schmidely, P., Demersay, T.-C., Azzout-Marniche, D., 2020. Histidine: a systematic review on metabolism and physiological effects in human and different animal species. Nutrients 12 (5), 1414. https://doi.org/10.3390/nu12051414.

Navas, J.M., Segner, H., 2006. Vitellogenin synthesis in primary cultures of fish liver cells as endpoint for in vitro screening of the (anti)estrogenic activity of chemical substances. Aquat Toxicol. 80 (1), 1–22. https://doi.org/10.1016/j.aquatox.2006.07.013.

Norwegian food safety authority, 2022. https://www.mattilsynet.no/planter_og_dyrking/genmodifisering/.

Olsvik, P.A., Søfteland, L., 2020. Mixture toxicity of chlorpyrifos-methyl, pirimiphos-methyl, and nonylphenol in Atlantic salmon (Salmo salar) hepatocytes. Toxicol Rep 7, 547–558. https://doi.org/10.1016/j.toxrep.2020.03.008.

Olsvik, P.A., Berntssen, M.H., Søfteland, L., 2015. Modifying effects of vitamin e on chlorpyrifos toxicity in Atlantic salmon. PLoS One 10, e0119250. https://doi.org/10.1371/journal.pone.0119250.

Olsvik, P.A., Søfteland, L., Hevrøy, E.M., Rasinger, J.D., Waagbø, R., 2016. Fish pre-acclimation temperature only modestly affects cadmium toxicity in Atlantic salmon hepatocytes. J. Therm. Biol. 57, 21–34. https://doi.org/10.1016/j.jtherbio.2016.02.003.

Olsvik, P.A., Berntssen, M.H.G., Søfteland, L., 2017. In vitro toxicity of pirimiphos-methyl in Atlantic salmon hepatocytes. Toxicol. Vitro 39, 1–14. https://doi.org/10.1016/j.tiv.2016.11.008.

Ørnsrud, R., Silva, M., Berntssen, M., Lundebye, A.-K., Storesund, J., Lie, K.K., Waagbø, R., Sele, V., 2020. Monitoring program for fish feed. Annual report for samples retrieved in 2019. ISSN: 1893-4536., 2020-34.

PubChem database, 2021. Available: https://PubChem (nih.gov).

Remø, S.C., Hevrøy, E.M., Olsvik, P.A., Fontanillas, R., Breck, O., Waagbø, R., 2014. Dietary histidine requirement to reduce the risk and severity of cataracts is higher than the requirement for growth in Atlantic salmon smolts, independently of the dietary lipid source. Br. J. Nutr. 111, 1759–2177. https://doi.org/10.1017/S0007114513004418.

Repetto, G., del Peso, A., Jorge L Zurita, J.L., 2008. Neutral red uptake assay for the estimation of cell viability/cytotoxicity. Nat. Protoc. 3, 1125–1131. https://doi.org/10.1038/nprot.2008.75.

Samanta, P., Mukherjee, A.K., Pal, S., Kole, D., Ghosh, A.R., 2016. Toxic effects of glyphosate-based herbicide, Excel Mera 71 on gill, liver, and kidney of Heteropneustes fossilis under laboratory and field conditions. J. Microsc. Ultrastruct. 4 (3), 147–155. https://doi.org/10.1016/j.jmau.2016.01.002.

Sanden, M., Olsvik, P.A., Søfteland, L., Rasinger, J.D., Rosenlund, G., Garlito, B., Ibanez, M., Berntssen, M.H.G., 2018. Dietary pesticide chlorpyrifos-methyl affects arachidonic acid metabolism including phospholipid remodeling in Atlantic salmon (Salmo salar L.). Aquaculture 484, 1–12. https://doi.org/10.1016/j.aquaculture.2017.10.033.

Schnellmann, R.G., 2008. Toxic responses of the kidney. In: Klaassen, C.D. (Ed.), Casarett and Doull's Toxicology: the Basic Science of Poisons. McGraw-Hill Companies, New York, pp. 583–608.

Schönbrunn, E., Eschenburg, S., Shuttleworth, W.A., Schloss, J.V., Amrheini, N., Evans, J.N.S., Kabsch, W., 2001. Interaction of the herbicide glyphosate with its target enzyme 5-enolpyruvylshikimate 3-phosphate synthase in atomic detail. Proc. Natl. Acad. Sci. U. S. A. 98 (4), 1376–1380. https://doi.org/10.1073/pnas.98.4.1376.

Schroeder, A., Mueller, O., Stocker, S., Salowsky, R., Leiber, M., Gassmann, M., Lightfoot, S., Menzel, W., Granzow, M., Ragg, T., 2006. The RIN: an RNA integrity number for assigning integrity values to RNA measurements. BMC Mol. Biol. 7, 3. https://doi.org/10.1186/1471-2199-7-3.

Schutte, M., Fox, B., Baradez, M.-O., Devonshire, A., Minguez, J., Bokhari, M., Przyborski, S., Marshall, D., 2011. Rat primary hepatocytes show enhanced performance and sensitivity to acetaminophen during three-dimensional culture on a polystyrene scaffold designed for routine use. Assay Drug Dev. Technol. 9 (5), 475–486. https://doi.org/10.1089/adt.2011.0371.

Segner, H., Braunbeck, T., 2003. End points for in vitro toxicity testing with fish cells. In: Mothersill, C., Austin, B. (Eds.), In Vitro Methods in Aquatic Toxicology. Springer, Chichester, UK, pp. 77–141.

Sele, V., Berntssen, M., Philip, A., Lundebye, A.-K., Lie, K.K., Espe, M., Storesund, J., Ørnsrud, R., 2021. Monitoring program for fish feed. Annual report for samples retrieved in 2020 (2021–28).

Shiogiri, N.S., Paulino, M.G., Carraschi, S.P., Baraldi, F.G., Cruz, C., Marisa Narciso Fernandes, M.N., 2012. Acute exposure of a glyphosate-based herbicide affects the gills and liver of the Neotropical fish, Piaractus mesopotamicus. Environ. Toxicol. Pharmacol. 34 (2), 388–396. https://doi.org/10.1016/j.etap.2012.05.007.

Sinensky, M., 1974. Homeoviscous adaptation - homeostatic process that regulates viscosity of membrane lipids in escherichia-coli. Proc. Natl. Acad. Sci. U. S. A. 71, 522–525, 1010.1073/pnas.71.2.522.

Søfteland, L., Eide, I., Olsvik, P.A., 2009. Factorial design applied for multiple endpoint toxicity evaluation in Atlantic salmon (Salmo salar L.) hepatocytes. Toxicol. Vitro 23, 1455–1464. https://doi.org/10.1016/j.tiv.2009.07.014.

Søfteland, L., Holen, E., Olsvik, P.A., 2010. Toxicological Application of Primary Hepatocyte Cell Cultures of Atlantic Cod (Gadus morhua) - Effects of BNF, PCDD and Cd. Comp. Biochem. Physiol. C Toxicol. Pharmacol. 151 (4), 401–411. https://doi.org/10.1016/j.cbpc.2010.01.003.

Søfteland, L., Petersen, K., Stavrum, A.K., Wu, T., Olsvik, P.A., 2011. Hepatic in vitro toxicity assessment of PBDE congeners BDE47, BDE153 and BDE154 in Atlantic salmon (Salmo salar L.). Aquat. Toxicol. 105 (3–4), 246–263. https://doi.org/10.1016/j.aquatox.2011.03.012.

Søfteland, L., Kirwan, J.A., Hori, T.S.F., Størseth, T.R., Sommer, U., Berntssen, M.H.G., Viant, M.R., Rise, M.L., Waagbø, R., Torstensen, B.E., Booman, M., Olsvik, P.A., 2014. Toxicological effect of single contaminants and contaminant mixtures associated with plant ingredients in novel salmon feeds. Food Chem. Toxicol. 73, 157–174. https://doi.org/10.1016/j.fct.2014.08.008.

Stegeman, J.J., Hahn, M.E., 1994. Biochemistry and molecular biology of monooxygenase: current perspectives on forms, functions and regulation of cytochrome P450 in aquatic species. In: Malins, D.C., Ostrander, G.K. (Eds.), Aquatic Toxicology: Molecular, Biocheimcal, and Cellular Perspectives. Lewis Publishers, Boca Raton, pp. 87–206.

Sung, J.H., Esch, M.B., Prot, J.-M., Long, C.J., Smith, A., Hickman, J., Shuler, M.L., 2013. Microfabricated mammalian organ systems and their integration into models of whole animals and humans. Lab Chip 13 (7), 1201–1212. https://doi.org/10.1039/c3lc41017j.

Tadaishi, M., Toriba, Y., Shimizu, M., Kobayashi-Hattori, K., 2018. Adenosine stimulates hepatic glycogenolysis via adrenal glands-liver crosstalk in mice. PLoS One 13 (12), e0209647. https://doi.org/10.1371/journal.pone.0209647.

Taub, M., 2005. Primary kidney proximal tubule cells. In: Helgason, C.D., Miller, C.L. (Eds.), Basic Cell Culture Protocols. Methods in Molecular Biology, vol. 290. Humana Press, Totowa, NJ., USA. https://doi.org/10.1385/1-59259-838-2:231.

Tellmann, G., 2006. The E-Method: a highly accurate technique for gene-expression analysis. Nat. Methods 3. https://doi.org/10.1038/nmeth894.

Tocher, D.R., 2003. Metabolism and functions of lipids and fatty acids in teleost fish. Rev. Fish. Sci. 11 (2), 107–184. https://doi.org/10.1080/713610925.

Torstensen, B.E., Frøyland, L., Lie, Ø., 2001. Lipider. In: Waagbø, R., Espe, M., Hamre, K., Lie, Ø. (Eds.), Fiskeernæring. Kystnæringen Forlag Og Bokklubb AS. Bergen, Norway, pp. 57–75.

Ueda, N., Tsuboi, K., Uyama, T., 2013. Metabolism of endocannabinoids and related N-acylethanolamines: canonical and alternative pathways. FEBS J. 280, 1874–1894. https://doi.org/10.1111/febs.12152.

van Timmeren, M.M., van den Heuvel, M.C., Bailly, V., Bakker, S.J., van Goor, H., Stegeman, C.A., 2007. Tubular kidney injury molecule-1 (KIM-1) in human renal disease. J. Pathol. 212, 209–217.

Vandesompele, J., Preter, K.D., Pattyn, F., Poppe, B., Roy, N.V., Paepe, A.D., Speleman, F., 2002. Accurate normalization of real-time quantiative RT-PCR data by geometric averaging of multiple internal control genes. Genome Biol. 3 (7) https://doi.org/10.1186/gb-2002-3-7-research0034. Research0034.1-0034.11.

Varga, T., Czimmerer, Z., Nagy, L., 2011. PPARs are a unique set of fatty acid regulated transcription factors controlling both lipid metabolism and inflammation. Biochim. Biophys. Acta 1812 (8), 1007–1022. https://doi.org/10.1016/j.bbadis.2011.02.014.

Vinken, P., Starckx, S., Barale-Thomas, E., Looszova, A., Sonee, M., Goeminne, N., Versmissen, Loes, Buyens, K., Lampo, A., 2012. Tissue Kim-1 and urinary clusterin as early indicators of cisplatin-induced acute kidney injury in rats. Toxicol. Pathol. 40 (7), 1049–1062. https://doi.org/10.1177/0192623312444765.

Wang, R., Chen, J., Ding, F., Zhang, L., Wu, X., Wan, Y., Hu, J., Zhang, X., Wu, Q., 2021. Renal tubular injury induced by glyphosate combined with hard water: the role of cytosolic phospholipase A2. Ann. Transl. Med. 9 (2), 130. https://doi.org/10.21037/atm-20-7739.

Webster, T.M.U., Laing, L.V., Florance, H., Santos, E.M., 2014. Effects of glyphosate and its formulation, Roundup, on reproduction in zebrafish (Danio rerio). Environ. Sci. Technol. 48 (2), 1271–1279. https://doi.org/10.1021/es404258h.

Xi, Y., Zhang, Y., Zhu, S., Luo, Y., Xu, P., Huang, Z., 2020. PPAR-mediated toxicology and applied pharmacology. Cells 9 (2), 352. https://doi.org/10.3390/cells9020352.

Zhu, C., Solorzano, C., Sahar, S., Realini, N., Fung, E., Sassone-Corsi, P., Piomelli, D., 2011. Proinflammatory stimuli control N-acylphosphatidylethanolamine-specific phospholipase D expression in macrophages. Mol. Pharmacol. 79, 786–792. https://doi.org/10.1124/mol.110.070201.